AN EXPERIMENTAL STUDY OF IMMERSED COIL HEAT EXCHANGERS

by

THOMAS JAMES FEIEREISEN

A thesis submitted in partial fulfillment of the
requirements for the degree of

MASTER OF SCIENCE
(Mechanical Engineering)

at the

UNIVERSITY OF WISCONSIN-MADISON

1982

ACKNOWLEDGMENTS

I am very grateful for the opportunity to have worked under the guidance of Professors J. A. Duffie and S. A. Klein. I would also like to direct my gratitude towards Professors W. A. Beckman and J. W. Mitchell for their frequent and helpful contributions. The staff and fellow graduate students of the Solar Energy Laboratory deserve much credit for their assistance - both academically and socially. I would like to extend sincere appreciation to Mark, Jerry, Daryl, and Mike - without their friendship and help, my graduate studies would have been far less rewarding.

A special thanks goes to my parents for their continual encouragement throughout my academic career - and to Kristina who provided comfort and hope.

Funding for this research was provided by the A. O. Smith Company and the University of Wisconsin Graduate School.

ABSTRACT

Solar water heating systems often use immersed coils (internal heat exchangers) located at or near the bottom of a thermal storage tank. This thesis discusses the results of an experimental study of four immersed coil configurations. The performance data are presented in the form of Nusselt number as a function of Rayleigh number. Other coil parameters such as effectiveness, internal and external convection heat transfer coefficients, wall thermal resistance and the overall heat-transfer coefficient-area product are also looked at. Methods for analysis of immersed coils are presented and some schemes to enhance the performance of immersed coils are explored and discussed. A simple computer model of a coil/storage tank system is presented and the output is compared to experimental data. Observations of coil performance are presented along with design suggestions.

TABLE OF CONTENTS

Table of Contents (continued)

LIST OF FIGURES

List of Figures (continued)

LIST OF TABLES

NOMENCLATURE

Symbols used in this thesis which do not appear below are defined locally in the text.

A_c	contact area
A_i	coil inside surface area
A_o	coil outside surface area
A_T	storage tank surface area (exposed to environment)
C_c	capacity rate of fluid on cold side, $\dot{m}C_{pc}$
C_h	capacity rate of fluid on hot side, $\dot{m}C_{ph}$
C_{min}	minimum capacity rate
C_p	specific heat
D_i	inside tube diameter
D_o	outside tube diameter
fxLMTD	fractional log-mean temperature difference
F_R'/F_R	heat exchange penalty factor
F_RU_L	negative slope of the collector efficiency curve
g	acceleration of gravity
Gr	Grashof number
h	convection heat-transfer coefficient
h_c	contact coefficient
h_i	inside convection heat-transfer coefficient
h_o	outside convection heat-transfer coefficient
k	thermal conductivity

Nomenclature (continued)

LMTD	log-mean temperature difference
m	mass of thermal storage
$\dot{m}$	fluid mass flow rate
Nu	Nusselt number
NTU	number of transfer units
Pr	Prandtl number
q	heat transfer rate
q_{max}	maximum possible heat transfer rate
q_{Tot}	total heat transfer rate
Ra	Rayleigh number
R_w	coil wall thermal resistance
t	time
T_c	temperature of the water in the coil
$T_{c,i}$	temperature of the fluid entering the cold side of the heat exchanger (Chapter 6)
$T_{c,o}$	temperature of the fluid leaving the cold side of the heat exchanger (Chapter 6)
T_f	film temperature
$T_{h,i}$	temperature of the fluid entering the hot side of the heat exchanger (Chapter 6)
$T_{h,o}$	temperature of the fluid leaving the hot side of the heat exchanger (Chapter 6)
T_ℓ	temperature of the coil water at a given point
T_o	temperature at time 0.
T_s	coil exterior surface temperature

Nomenclature (continued)

T_T	storage tank bulk temperature
T_∞	environment temperature
U	overall heat-transfer coefficient (or: overall loss coefficient)
UA	overall heat-transfer coefficient-area product

Greek Symbols

α	thermal diffusivity
β	volume coefficient of expansion
ΔT_i	temperature difference at the heat exchanger inlet
ΔT_o	temperature difference at the heat exchanger outlet
ΔT_x	temperature difference between the coil exterior surface and the storage tank water
ε	immersed coil effectiveness
μ	dynamic viscosity
ν	kinematic viscosity

1.0 Introduction and Literature Review

1.1 Introduction

Immersed coils are heat exchangers that generally lie at or near the bottom of a thermal storage tank containing a liquid. Another liquid is circulated through the coil, transferring its energy to the tank liquid. Thus, a forced convection heat transfer situation occurs inside the coil while free convection is the dominant mode of heat transfer from the exterior surface of the coil. Applications for immersed coil heat exchangers range from residential solar water heating systems to temperature control of industrial baths. The purpose of this study is to gain insight into coil performance in solar water heating systems.

The phenomenon of forced convection inside a tube has been well studied and standard correlations [1] can be used to predict heat transfer from the coil fluid to the coil wall. Free convection heat transfer from the exterior of these immersed coils is not well documented. This problem exists mainly because of the wide variety of possible geometries immersed heat exchanger coils may have.

The goals of this study are:

1) to investigate methods to improve the performance of immersed coils,
2) to present a method to quantify the performance of immersed coils, (heat transfer correlations for four immersed coil

configurations are presented),

3) to evaluate the accuracy of TRNSYS, transient system simulation program [2] in the modeling of thermal storage tanks with immersed coils, and

4) to relate some observations of immersed coil characteristics.

The heat transfer correlations are in the form of Nusselt number as a function of Rayleigh number. The data to formulate these correlations were obtained from a series of experiments conducted to cover the range of operating conditions normally found in residential solar water heating systems. The computer model simulation is performed by comparing the output of a TRNSYS storage tank model simulation to the data collected from an experimental storage tank system. Both a load draw and a no-load draw condition were simulated and compared with experimental measurements.

1.2 Literature Search

A literature search turned up very little useful data. A paper from the Ford Products Corporation [3] describes a method to determine the effectiveness of one of their immersed coils (surface area = 0.93 m^2, configuration: flat spiral). The method consists of finding the number of transfer units, NTU, of the coil based on the coil fluid flow rate, the surface area of the coil and the overall heat-transfer coefficient obtained from curves produced from experimental data. The value of coil effectiveness is then found from the equation:

$$\varepsilon = 1 - \exp\,[-NTU] \qquad 1.2.1$$

The Ford Product method predicts an effectiveness for the horizontal, multi-pass, smooth-tube coil (described in Chapter 2) of about 25% below that which is measured. An obvious reason for this discrepancy is the difference between the two coil configurations. Another reason is that one must estimate the energy collected during a typical or average hour. What is typical or average can cover a wide range depending on many operating factors. The value of energy collected in an average hour for this comparison was the average measured over a period of about 8 hours.

A report from the Vaughn Corporation [4] gives performance data for a specific heat exchanger coil (finned tube; configuration is not described). A comparison between the data of this report and the data obtained in this study is not possible because the data is for exchangers of specific surface area with no provisions to estimate performance of coils with different surface areas.

A more general study of the development of heat transfer correlations for horizontal, straight, finned tubes is presented in a paper by Wiebelt, Henderson and Parker [5]. This paper presents useful general data regarding finned tube performance and a method of analysis, but is not comparable to the data collected in this study due to the marked difference between the finned coil configuration used in this study (a horizontal spiraling type described and shown in Chapter 2) and the horizontal, straight, finned tube coil

mentioned above.

P. J. Lunde [6] presents the equation*

$$h = 142. \left(\frac{\Delta T_x}{D_o}\right)^{0.25} \qquad 1.2.1$$

where: h is the convection heat transfer coefficient in $W/m^2{}^\circ C$.

ΔT_x is the temperature difference between the coil and the storage tank bulk temperature.

D_o is the characteristic length of the coil (which in this case is 1/2 the tube circumference).

Lunde explains that this equation has solid theoretical roots but has not been verified through experiments. It is described by Lunde to be useful for in-tank or traced-tank coils but is based on free convection heat transfer correlations for straight, horizontal tubes [7]. A comparison of equation 1.2.1 with actual experimental data obtained from tests of two coil configurations (the horizontal, multi-pass, smooth-tube coil and the single-pass, smooth-tube coil; both described in Chapter 2) is plotted in Figure 1.2.1. Lunde's equation appears to over predict the heat transfer coefficient of the multi-pass coil by about 30%. Predictions for the single pass coil are low. Equations of this type seem to be rather specific.

---

*Equation 1.2.1 applies when the average of the coil and tank temperature is 38.°C. For 65.°C, multiply by 1.15; for 21.°C, multiply by 0.80. Much below that natural convection is weak, ceasing entirely below 4.°C, the maximum density of water.

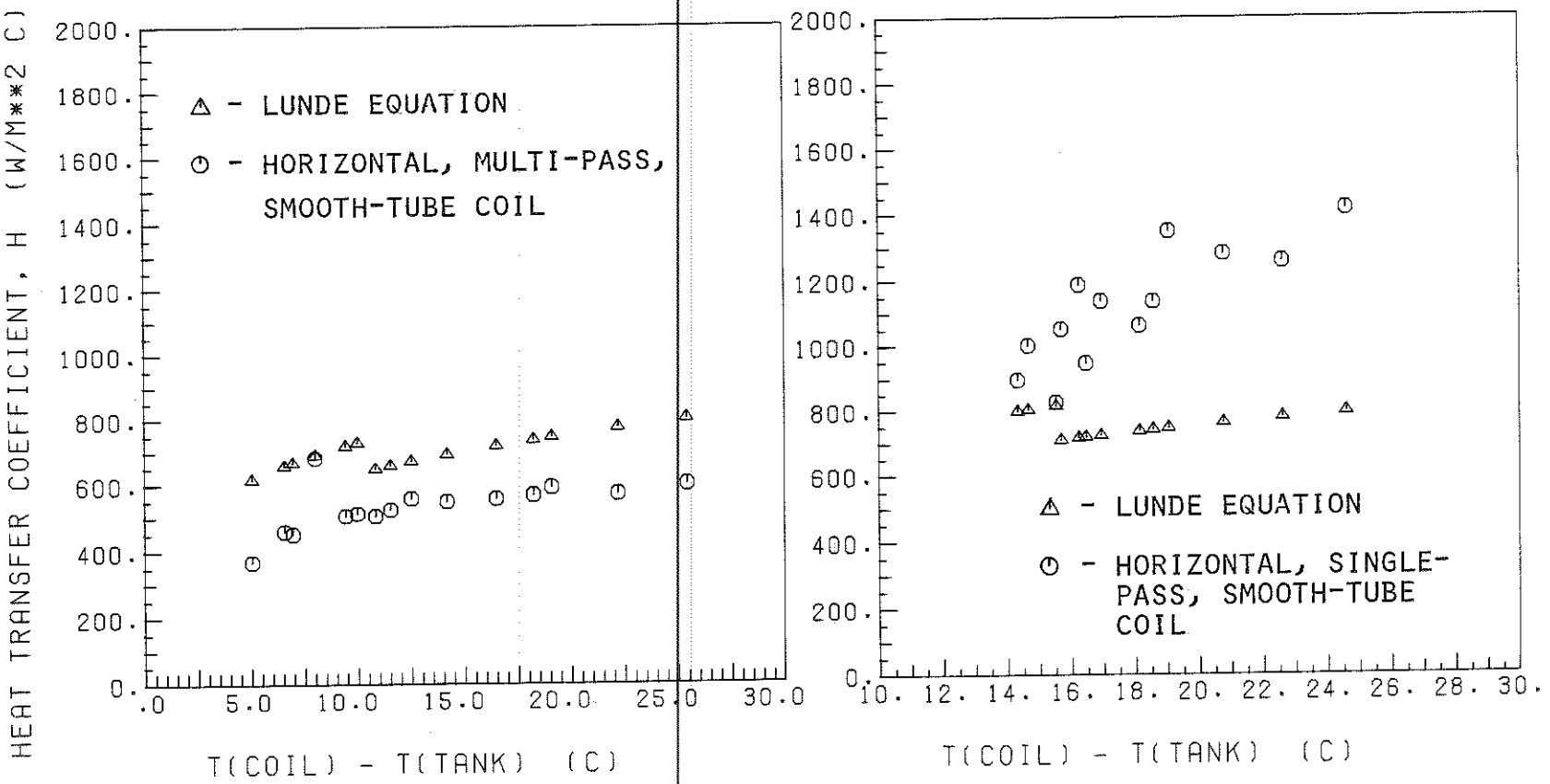

Figure 1.2.1 A comparison of Lunde's equation for the heat-transfer coefficient, h, and the experimentally measured value of h

Each type of coil configuration would need a specific equation to accurately describe its performance. A general equation such as that of equation 1.2.1 will oftentimes produce large errors in performance predictions.

A report written by Horel and de Winter [8] describes the development of design parameters and a method to determine optimum tube length for the helical coil. Their methods were not explored in this study since no helical coils were readily available to fit the storage tank used in this study.

2.0 Physical Description and Experimental Procedure

2.1 The Experimental System

The experimental apparatus is shown in Figure 2.1.1. The hot water source is a 300 liter water heater with a 3 kw electric resistance heater.

The water storage tank (thermal storage tank) is a 340 liter, 1.40 m high by 0.62 m diameter solar water heater tank with an internal, immersed coil. Fittings located on the top allow water to be drawn off and replaced and permit access for instrumentation. The immersed coils are connected through plates which bolt over access portals in the side of the tank. Tank insulation is provided by a 0.06 m fiberglass sheath. The whole unit is enclosed in a 0.8 mm thick steel case. The overall-loss coefficient (also called overall heat-transfer coefficient), U, has been experimentally determined to be 0.89 $W/m^2{}^\circ C$ (see section 6.2) based on an average tank temperature of 55.°C and an average environment temperature of 19.°C. There are negligible losses occurring through the bottom of the tank due to added insulation measures. There is a dead-air space between the tank bottom and the outer case bottom. The tank also rests on top of a 0.04 m thick polystyrene board. Therefore the bottom surface is neglected in heat transfer calculations involving the tank and the environment. The storage tank specifications are given in Appendix A.

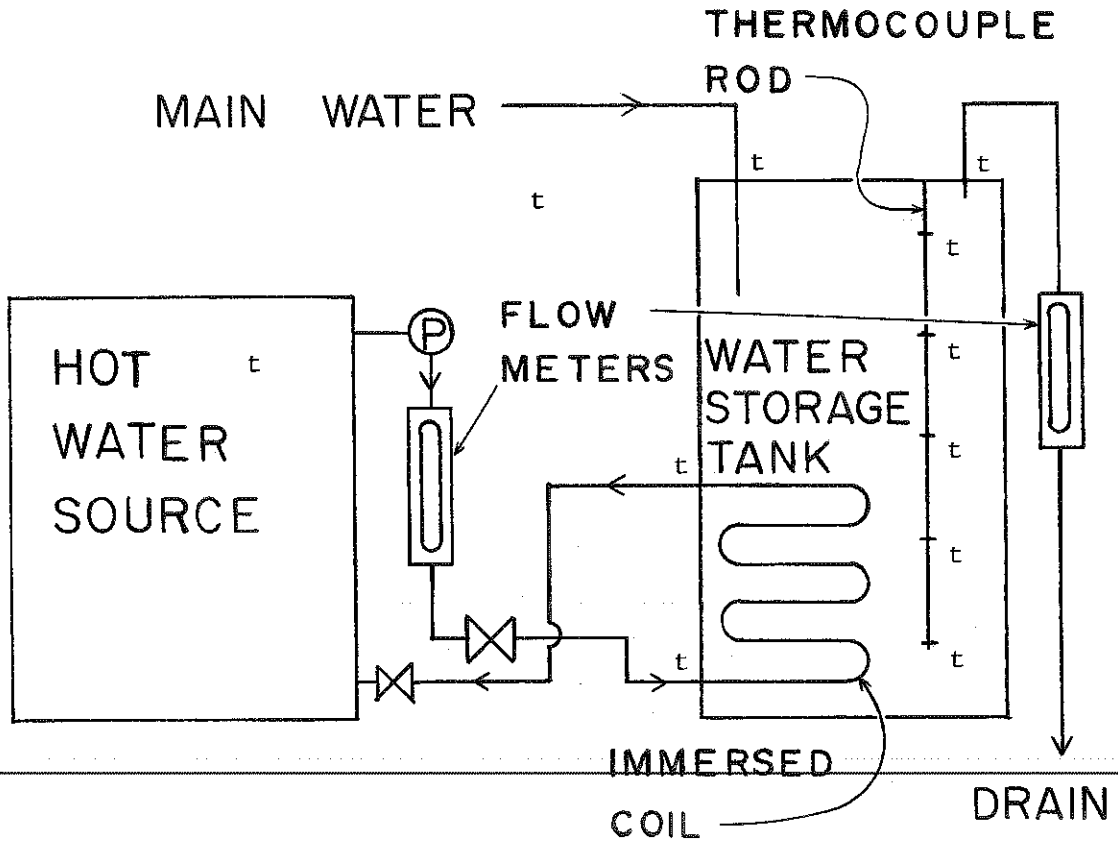

Figure 2.1.1 System diagram

(t → represents thermocouple location)

The coil assembly of the water storage tank is removable and interchangeable via portals on the storage tank side. Three types of immersed coils (shown in Figure 2.1.2 and described in Table 2.1.1) were investigated. They are:

1) horizontal, multi-pass, smooth-tube coil (4 passes),

2) horizontal, spiraling, finned-tube coil, and

3) horizontal, single-pass, smooth-tube coil.

All three coil types are made of copper. Coil types 1 and 2 have double-wall construction to meet building codes in some states regarding contamination of potable water with the heat transfer fluid within the coil. The double-wall construction is simply a tube inside a tube with close tolerances. The unit is then crimped along its length to form a press-fit. Coil type 3 has single-wall construction. A fourth coil configuration consisting of two type 1 coils connected in series and mounted one above the other (0.2 meters apart, the lower coil being mounted 0.2 meters above the bottom of the tank) was also investigated.

The average wall thermal resistances for each of the four coil configurations is given in Table 2.1.2. The values of wall thermal resistance of the double-wall coils are based on the measured contact coefficients at the interface of the double-walls. The method used to determine the contact coefficients is presented in Appendix C.

The effect of coil orientation was investigated using the single-pass, smooth-tube coil shown in Figure 2.1.2c modified to be inclined at angles of 0°, 45°, and 90° from horizontal. In these

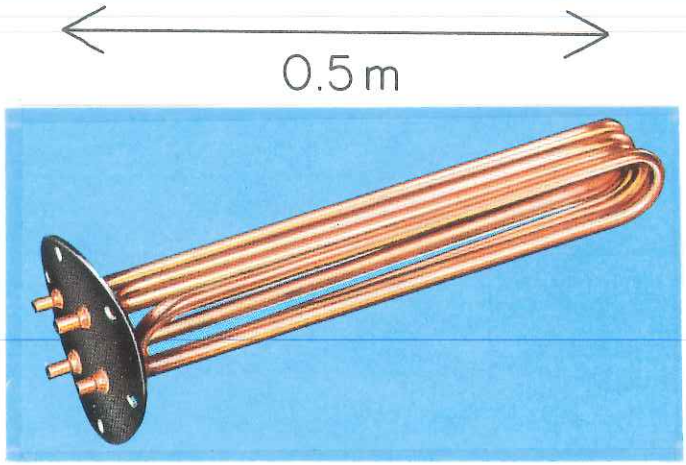

a) horizontal, multi-pass smooth-tube coil

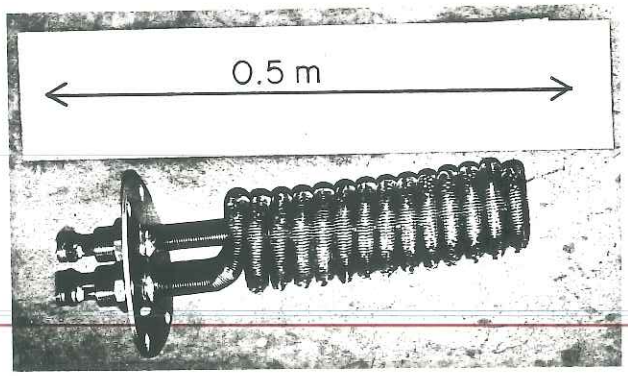

b) horizontal, spiraling, finned-tube coil

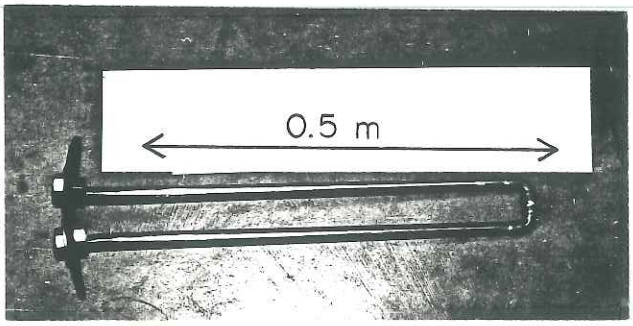

c) horizontal, single-pass, smooth-tube coil

Figure 2.1.2 Immersed coils

Table 2.1.1 Coil Specificiations

PROPERTY	HORIZONTAL, MULTI-PASS, SMOOTH-TUBE COIL	HORIZONTAL, SPIRALING, FINNED-TUBE COIL	HORIZONTAL, SINGLE-PASS SMOOTH-TUBE COIL
OVERALL LENGTH	0.55 m	0.38 m	0.54 m
OVERALL WIDTH	0.08 m	0.09 m	0.07 m
OVERALL HEIGHTH	0.08 m	0.09 m	0.016 m
TUBE DIA.-OUT	0.016 m	0.0145 m	0.016 m
TUBE DIA.-IN	0.011 m	0.011 m	0.015 m
TUBE LENGTH	4.50 m	3.56 m	1.11 m
FIN DIA.	--	0.0213 m	--
AREA-OUT	0.225 m^2	0.73 m^2	0.057 m^2
AREA-IN	0.155 m^2	0.12 m^2	0.051 m^2
MATERIAL	Cu	Cu	Cu
CONSTRUCTION	DOUBLE WALL	DOUBLE WALL	SINGLE WALL
CHARACTERISTIC DIMENSION	0.016 m	0.0145 m	0.016 m

Table 2.1.2 Average Wall Resistance for the Four Coil Configurations

Configuration	Wall Resistance	How Obtained?
Horizontal, multi-pass smooth-tube coil (2 coils)	2.3×10^{-3} °C/W	Measured
Horizontal, multi-pass smooth-tube coil (1 coil)	4.7×10^{-3} °C/W	Measured
Horizontal, spiraling finned-tube coil	1.8×10^{-3} °C/W	Measured
Horizontal, single-pass, smooth-tube coil	3.1×10^{-5} °C/W (negligible)	Calculated

tests, the lowest position on the coil was located 0.4 meters from the bottom of the tank. Identical tests were conducted for each of the three coil inclinations to obtain performance comparisons.

A small centrifugal, liquid pump rated at 370 watts was used to obtain coil volumetric flow rates up to 0.150 ℓ/s (typical of residential solar water heating applications). A second pump, identical to the previously described one, was used for several sets of experiments involving forced convection on the exterior of the immersed coil. Typically, water was drawn out of the tank and then pumped back in some fashion to create a flow within the tank. Fluid volume flows were measured with two rotameters; one placed in the source tank-immersed coil loop and the other in the load line from the storage tank. The coil volumetric flow rates are accurate to within about $\pm$5%.

A chart recorder with 12 channels was used to log temperature data obtained with Cu-Cn thermocouples at the 11 locations shown in Figure 2.1.1. The locations of the thermocouples are:

1-5) equally spaced within the storage tank from bottom to top;

6) immersed coil, in;

7) immersed coil, out;

8) hot water source tank;

9) environment;

10) water storage tank, in; and,

11) water storage tank, out.

The five thermocouples within the tank are equally spaced so that the average temperature recorded from these is the bulk temperature of the storage tank. Fluid mixing devices were constructed and placed in the piping at points of temperature measurement to obtain the bulk temperature of the flows. Temperature measurements are estimated to be accurate to within $\pm 0.3°C$.

For some of the early experiments, a mercury manometer was connected across the inlet and outlet of the coil. The pressure drop was measured at various coil volumetric flow rates for the horizontal, multi-pass, smooth-tube coils (one coil and two coils connected in series). The manometer was disconnected early in the study due to continual leaks at the pressure taps.

2.2 General Experimental Procedure

All experiments conducted used tap water for both the immersed coil-source tank loop and the thermal storage tank. The water on both sides of the immersed coil was unsoftened.

The coil assembly to be tested was installed in the storage tank with the inlet and outlet connected to the hot water source tank. Fiberglass insulation was then placed over the coil mounting plates to maintain the original tank insulating properties.

Experiments were always started with a fully charged source tank; initially at about 72.°C. The temperature of the water going

into the coil was approximately the same. This delivery temperature varied over the course of an experiment as the storage tank heated up and the source tank cooled. When the source tank temperature dropped below 65.°C, the electric heater would turn on to heat the source tank. This action created a fluctuating temperature of the fluid entering the immersed coil. In a typical experiment, energy was delivered to the storage tank (initially at 10.°C - 15.°C) by circulating the hot source tank water through the heat exchanger coil. At the end of the experiment, the storage tank temperatures were generally in the 65.°C - 70.°C range. The volumetric flow rate through the coil was held constant during any given experiment, but a range of coil volumetric flow rates from 0.02 ℓ/s to 0.125 ℓ/s were used in different experiments. For most of the analysis, a flow rate of 0.075 ℓ/s to 0.125 ℓ/s was used to approximate rates used in residential solar water heating systems.

Further experiments involved the addition of a load to the storage tank by drawing hot water off the storage tank and replacing it with main water at ~10.°C. Each of these experiments consisted of several load draws at various flow rates although each load draw was at a constant volumetric flow rate. The variation of load draws was from 0.075 ℓ/s to 0.150 ℓ/s for a period of one-half hour. This was done to simulate heavy residential or light industrial hot water usage.

For the immersed coil performance enhancement experiments involving forced convection, a second 370 watt pump was used to obtain

a forced convection situation on the exterior side of the immersed coil. The maximum volumetric flow rate obtainable with this pump and with the pressure loss of the piping was ~0.30 ℓ/s. The maximum flow rate was used for all experiments involving forced convection on the exterior coil surface.

When measuring the overall-loss coefficient, U of the storage tank, the initial temperature of the storage tank was 52.8°C. The tank was allowed to cool (only through losses from the storage tank surface exposed to the environment) to a temperature of 40.4°C after 55 hours. The coil was not operating during these measurements. For all experiments, temperatures and coil volumetric flow rates were monitored for the duration of an experiment, typically 12-24 hours. The maximum rate of temperature change recorded in the system was the source tank temperature during the beginning portion of each test. The maximum rate of change was approximately 8°C per hour and was usually much less. After three hours, the maximum rate of temperature change was on the order of 3°C/hr or less. Due to this relatively low rate of temperature change, the temperatures measured at a given time could be considered steady-state.

3.0 Problems Encountered During Data Acquisition

Certain problems and quirks in the system surfaced during the experiments. This section describes these problems and discusses methods to eliminate them.

3.1 Temperature Measurements

3.1.1 Temperature Fluctuations of the Water Entering the Coil

As the storage tank heated up, the hot water source tank cooled down due to the transfer of thermal energy. The thermostat of the hot source water tank was set at 70.°C. Fluctuations in this control system along with the transfer of thermal energy to the storage tank produced fluctuations in the temperature of the water entering the immersed coil from 45.°C to 72.°C. These fluctuations in the temperature of the fluid entering the coil along with varying initial storage tank temperatures produced a wide range of temperature differences seen by a coil after the same time period in different experiments.

Comparisons between different tests of a coil were made by plotting the heat transfer rate as a function of the log-mean temperature difference over the same range of temperature difference between the immersed coil inlet and the storage tank temperature. The range of this temperature difference was from 5.°C to 50°C.

The best approximation of the data obtained at large temperature differences is a straight line. The actual heat transfer rate at low heat input rates may appear as follows [4]:

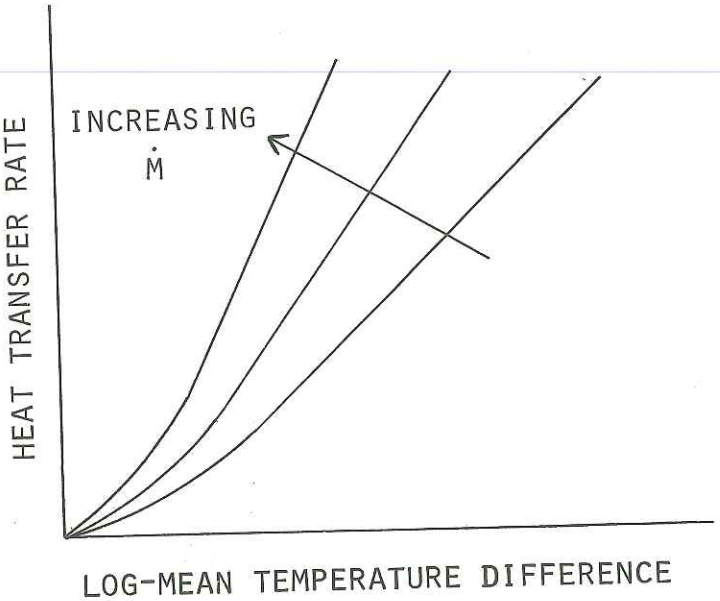

or:

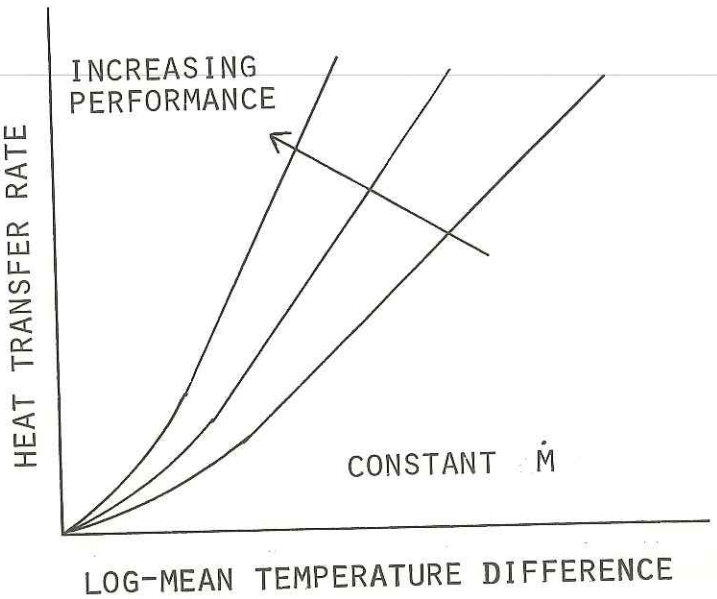

The greater the slope of this line, the greater the volumetric flow rate of the coil. Or at a constant coil volumetric flow rate (constant $\dot{m}$), the greater the slope of this line, the better the performance of the coil. For a given log-mean temperature difference, the heat-transfer rate of two or more coils operating under different conditions can be compared. This provides a comparison of performance between the coils.

3.1.2 Stratification Under Storage Tank Load Conditions

Stratification in the storage tank occurs during the period of a load draw. This stratification soon disappears when the load ceases. Oftentimes a measurement of the bulk storage tank temperature is needed for calculations during a period of stratification. The thermocouple rod located in the storage tank measures the temperature at the center of five equal-sized portions of water vertically situated between the top and bottom of the tank. An average of these five temperatures gives the bulk temperature of the water in the storage tank.

3.1.3 Small Temperature Differences Between the Inlet and Outlet of the Coil

When testing immersed coils with small surface areas, the temperature drop between the inlet and outlet is relatively small. This tends to create large errors. For instance, during a particular experiment, the volumetric flow rate through a horizontal,

multi-pass, smooth-tube coil (2 coils, connected in series, area = 0.45 m^2) was 0.125 ℓ/s. The temperature of the water entering the coil was 52.1°C and the temperature of the water leaving the coil was 42.2°C. The temperature drop is 9.9°C. Each temperature measurement is accurate to only about $\pm$ 0.3°C so the error of a temperature difference is twice that of a temperature measurement or $\pm$ 0.6°C. The maximum percent error expected would then be:

$$\frac{0.6°C}{9.9°C} = 6\% \text{ error,}$$

a relatively small percentage of error.

A second immersed coil (a horizontal, single-pass, smooth-tube coil; area = 0.057 m^2) also has water flowing through at 0.125 ℓ/s. The temperature of the water at the entrance is 60.2°C; at the exit, 57.1°C. Following the same analysis as above we find:

$$\frac{0.6°C}{3.1°C} = 19\% \text{ error.}$$

This becomes a rather large error. The maximum expected error involving temperature drop across the coil increases as the temperature drop decreases. The impact of this problem was reduced by relying more heavily on data obtained at lower coil volumetric flow rates and data obtained early in the experiment. The lower volumetric flow rates produce greater temperature differences between the inlet and

outlet of the coil and thus reduce the error. Early in an experiment, the storage tank bulk temperature is low. This means a larger temperature difference exists between the coil and the tank. This larger temperature difference also produces a greater temperature drop in the fluid passing through the coil which reduces the error. It is possible that some meaningful information present only at low temperature differences between the coil temperature and the tank temperature was overlooked because of this technique.

3.2 Poor Storage Tank Mixing

Tests conducted with heat exchangers of small surface area tended to leave the portion of the water under the coil relatively unaffected by the energy transfer. The convective currents around the smaller immersed coil were not sufficient to mix the water throughout the entire storage tank. All points in the storage tank above the coil were at approximately the same temperature ($\pm$ 1.0°C). For analysis purposes, the cooler lowest segment of the tank (that below the coil) was ignored. The bulk storage tank temperature was then taken to be the average of those temperatures measured above the coil. The error induced by ignoring the lower temperature of the water located below the coil is small since this segment of water makes up only about 5% of the mass of the water in the storage tank.

3.3 Other Assorted Problems

The water used in all experiments was unsoftened tap water. Over a period of a few months, significant mineral deposits would form on the exterior surface of the coil installed in the storage tank (see Figure 3.3.1). These deposits produced a small (<10%) decrease in immersed coil performance over a period of four months. Due to these deposits, experiments using the same coil could not be accurately compared if there was a significant time span between them (say one month). To alleviate this problem, experiments involving the same coil operating under different conditions were performed back to back. Then when comparing the data, the effects of mineral deposits are negligible since significant deposits take weeks or even months to accumulate. The immersed coils were cleaned of all deposits prior to obtaining the dimensionless data of Nusselt-Raliegh number relationships.

Certain other problems such as plugged or partial plugged plumbing or air in the coil-source tank loop required that an experiment be repeated.

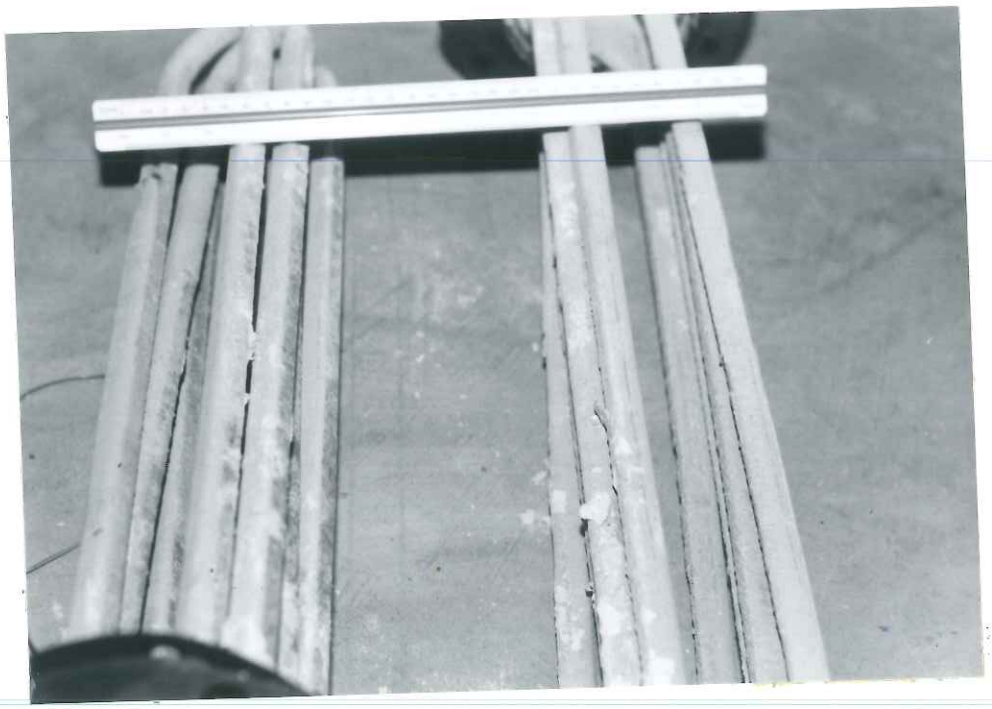

Figure 3.3.1 Mineral deposits on coil surface

4.0 Data Reduction

The temperature and immersed coil volumetric flow data were reduced to obtain the following information.

The heat exchanger effectiveness, ε, defined as:

$$\varepsilon = \frac{T_{c,in} - T_{c,out}}{T_{c,in} - T_T} \qquad 4.0.1$$

The instantaneous heat-transfer rate of the heat exchanger coil, q, defined as:

$$q = \dot{m} C_p (T_{c,in} - T_{c,out}) \qquad 4.0.2$$

Log-mean temperature difference, LMTD, which in this case is:

$$LMTD = \frac{T_{c,in} - T_{c,out}}{\ell n \frac{T_{c,in} - T_T}{T_{c,out} - T_T}} \qquad 4.0.3$$

The overall heat-transfer coefficient-area product, UA, defined as:

$$UA = \frac{q}{LMTD} \qquad 4.0.4$$

The average coil exterior convection heat-transfer coefficient h_o, as calculated from:

$$h_o = \frac{1}{A_o \left[\frac{1}{UA} - \frac{1}{h_i A_i} - R_w\right]} \qquad 4.0.5$$

The internal convection coefficient, h_i, and the coil wall resistance are determined experimentally by methods described in Appendix C. The internal convection coefficient may also be calculated (with less accuracy) from the Dittus-Boelter equation [1] for turbulent flow in smooth tubes.

Further data processing produced the Nusselt and Rayleigh numbers, defined as

$$Nu = \frac{h_o D_o}{k} \qquad 4.0.6$$

and

$$Ra = GrPr = \frac{g\beta(f \times LMTD) D_o^3}{\nu\alpha} \qquad 4.0.7$$

The quantity, f x LMTD is discussed below. Properties were evaluated at the film temperature, defined as the average of the storage tank temperature and the exterior coil surface temperature. The average exterior coil surface temperature was obtained from

$$T_s = T_T + \frac{q}{h_o A_o} \qquad 4.0.8$$

Evaluation of f x LMTD:

To evaluate the temperature difference between the surface of the coil and the bulk temperature of the tank we must use a log-mean

temperature difference. The log-mean temperature difference between the coil surface and the bulk tank temperature is some fraction, f of the log-mean temperature difference between the fluids on both sides of the heat exchanger coil. This relationship is shown in Figure 4.0.1. The fraction, f, is a function of the thermal resistance due to the free convection from the exterior of the immersed coil and the overall thermal resistance from the coil liquid to the storage tank water. Referring to Figure 4.0.1 and using the definition of the log-mean temperature difference, we have:

$$\frac{f \times \Delta T_i - f \times \Delta T_o}{\ell n \frac{f \times \Delta T_i}{f \times \Delta T_o}} = f \times LMTD \qquad 4.0.9$$

To evaluate the fraction, f, notice that the heat transfer rate from the coil fluid to the storage tank fluid is equal to the heat transfer rate from the coil wall to the storage tank fluid. So:

$$q_{overall} = q_{coil\ wall \rightarrow tank} \qquad 4.0.10$$

or, again referring to Figure 4.0.1, at a given point along the heat exchanger coil,

$$UA\ (T_\ell - T_T) = h_o A_o\ (T_s - T_T) \qquad 4.0.11$$

and

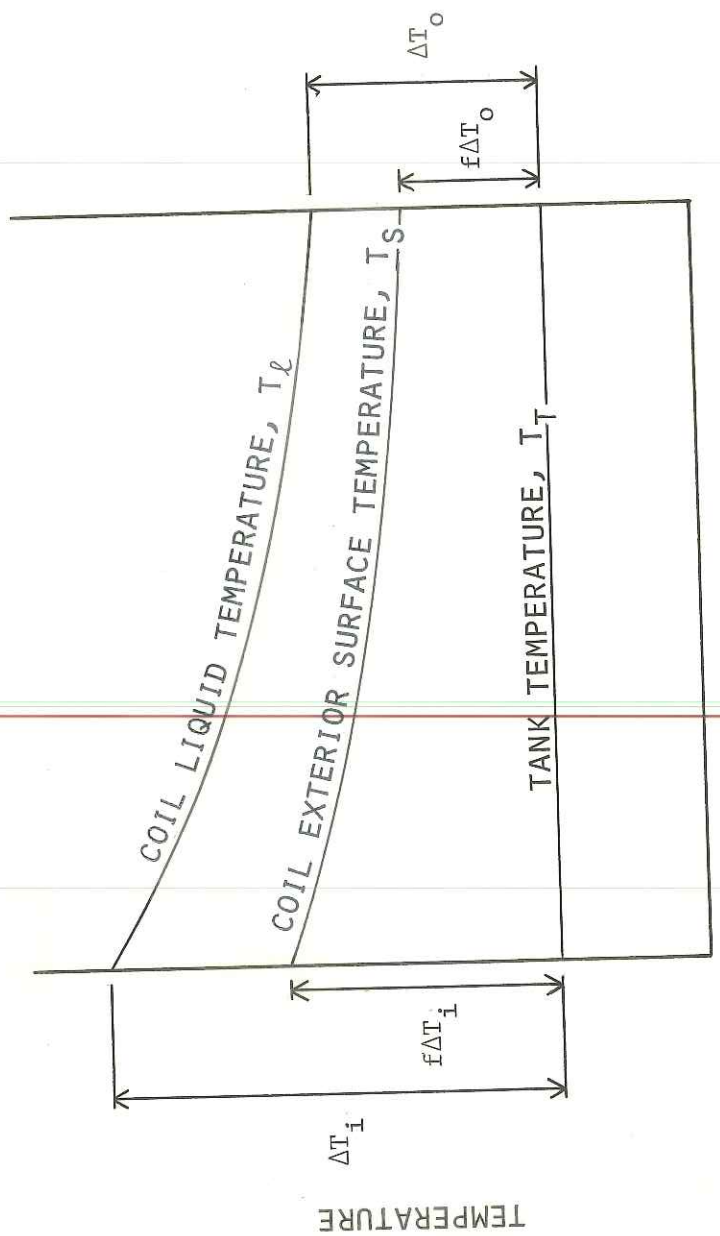

Figure 4.0.1 Fractional LMTD (f x LMTD)

$$f = \frac{T_s - T_T}{T_\ell - T_T} \qquad 4.0.12$$

Combining equations 4.0.11 and 4.0.12 we get,

$$f = \frac{UA}{h_o A_o} \qquad 4.0.13$$

This fractional log-mean temperature difference is an accurate way to describe the temperature difference between the coil wall and the tank fluid. The fraction, f, typically ranges from 0.40 to 0.55. This indicates that roughly 50% of the thermal resistance of the coil heat exchanger is due to the free convection mode of heat transfer at the coil exterior surface.

5.0 Experiments

This chapter describes the series of experiments conducted over the course of this project. The general procedure for conducting an experiment was given in Chapter 2; the specifics of each set of experiments are presented here. Each set of tests was conducted at various coil volumetric flow rates. Occasionally, a test was repeated to determine reliability of the data collected. In all cases, the repeatability of the test was high. The observations and results for each set of experiments are also presented. These observations and results will be summarized in the Discussion and Conclusions Chapter.

5.1 Coil Position

There are two mounting portals in the side of the storage tank and thus, there are two possible positions for a given coil to be mounted in the storage tank. The lower position is located 0.2 meters above the bottom of the tank and the upper position is located 0.4 meters above the bottom of the tank. In both positions, the mounted coil extends across the center of the tank. Two identical horizontal, multi-pass, smooth-tube coils (shown in Figure 2.1.2a) were mounted in the portals and each was tested separately to compare the effects of coil position.

The top position coil was tested first. Initial bulk tank temperatures were in the 10°C - 15°C range. The initial temperature of the water entering the coil was about 65°C but dropped off sharply (20°C) within the first hour of the experiments as the energy of the hot water source was depleted. The electric heater switched on at about 65°C and the temperature of the water entering the coil began to rise towards the 72°C set temperature of the source tank. Smaller fluctuations (~8.°C) in the entering fluid temperatures were observed thereafter as a result of the electric heater of the source tank turning off and on. Three volumetric flow rates of water through the coil were investigated; 0.079 ℓ/s, 0.095 ℓ/s and 0.11 ℓ/s. These volumetric flow rates are in the range of those used in residential solar water heating systems.

The same procedures were followed for the second, identical coil mounted in the lower position. Approximately the same initial temperatures for the coil inlet and the storage tank were encountered while testing both coils.

Results:

Figure 5.1.1 shows a comparison of an immersed coil mounted in the upper position with one mounted in the lower position. Within the errors of the measurements, both coil positions show the same performance. The horizontal, multi-pass, smooth-tube coil (in either mounting position) produces convective currents which are great

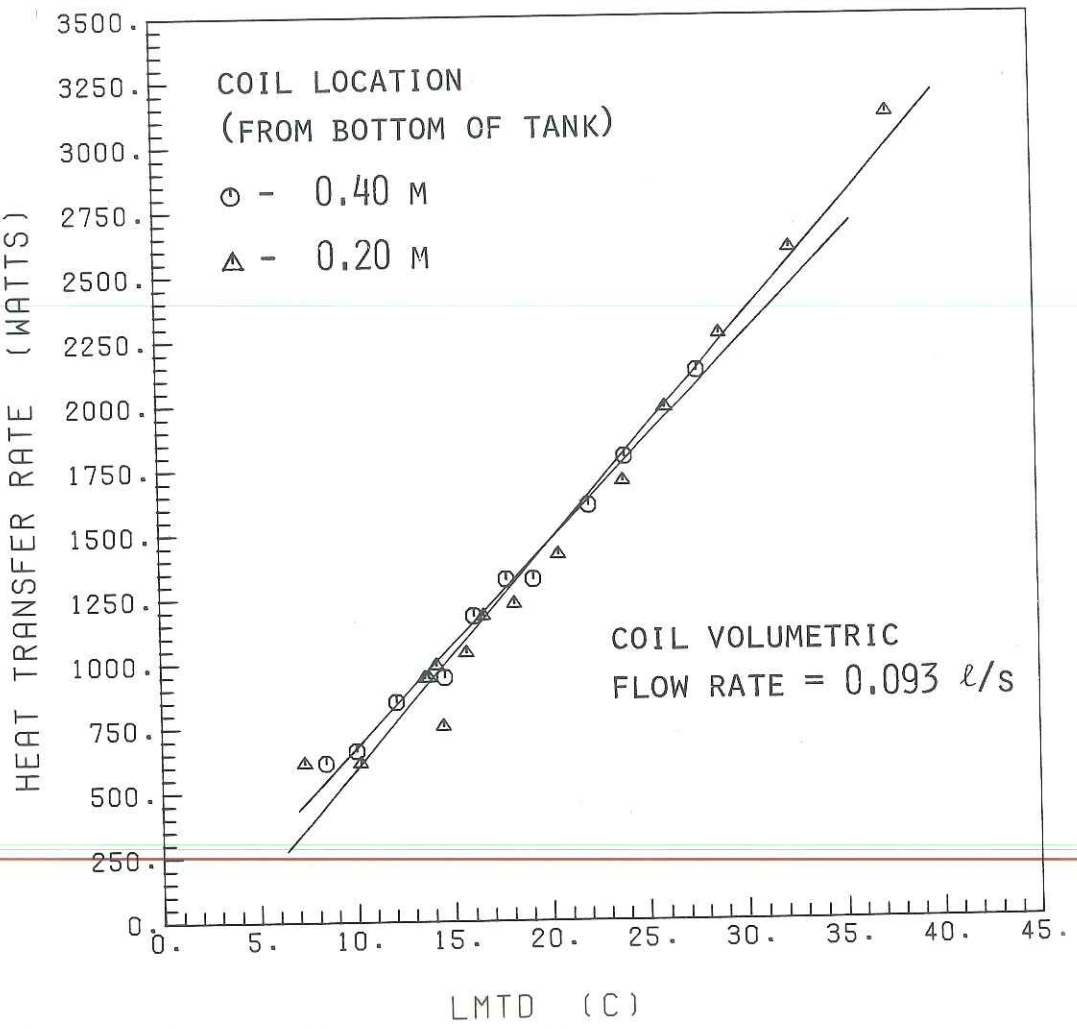

Figure 5.1.1 A comparison of immersed coil performance between two positions for the coil

enough to fully mix the water in the vicinity of the coil and at all points above it. Both positions of the coils see the same temperatures and therefore perform similarly. There is a cooler layer of water located at the bottom of the tank, below the coil when using both immersed coil positions. This layer is only minimally affected by the presence of the coil above it. The cooler layer is larger for the coil mounted in the upper position than the one mounted in the lower position. The lower mounted coil allows a greater utilization of the mass of the water for thermal storage than does the upper mounted coil.

5.2 Direction of Fluid Flow Within the Coil

Two horizontal, multi-pass, smooth-tube coils were mounted in the side portals of the storage tank. These two coils were then connected in series by adding a tube between the exit of one coil and the entrance of the other coil (the fourth coil configuration as described in Chapter 2). This produced one horizontal, multi-pass, smooth-tube coil of twice the area of the coil type 1 described in Chapter 2 (now 0.45 m^2). One end of the coil is located 0.17 m above the bottom of the tank and the other is located 0.43 m above the bottom. In the first series of tests, the upper end of the coil was connected to the outlet of the hot water source tank and the lower end of the coil connected to the inlet of the hot water source tank. In the following set of experiments, the plumbing con-

nections between the coil and the hot water source tank were reversed. By comparing the data from these two sets of tests, one can determine whether there is a difference in coil performance depending on the direction of the fluid flow through the coil.

For both sets of tests, water from the source tank was circulated through the coil a volumetric flow rate varying from 0.02 ℓ/s to 0.10 ℓ/s. The initial temperature of the water entering the coil was in the 65.°C - 70.°C range and varied during the tests by up to 15.°C. The initial tank bulk temperature for these tests was in the 10.°C - 15.°C range. The duration of each test was typically 10-12 hours.

Results:

The plumbing arrangement which allows the hot source water to enter at the lower end of the coil (0.17 m from the bottom of the tank) proved to be slightly superior to the arrangement allowing the hot source tank water to enter the upper end of the coil (0.43 m above the bottom of the tank). As seen in Figure 5.2.1 the output of the immersed coil is roughly 350.W greater for a given LMTD when the hot water enters the lower end of the coil rather than the upper end. The difference between the heat-transfer rates of the two flow configurations becomes a smaller fraction of the total heat-transfer rate as the log-mean temperature difference increases.

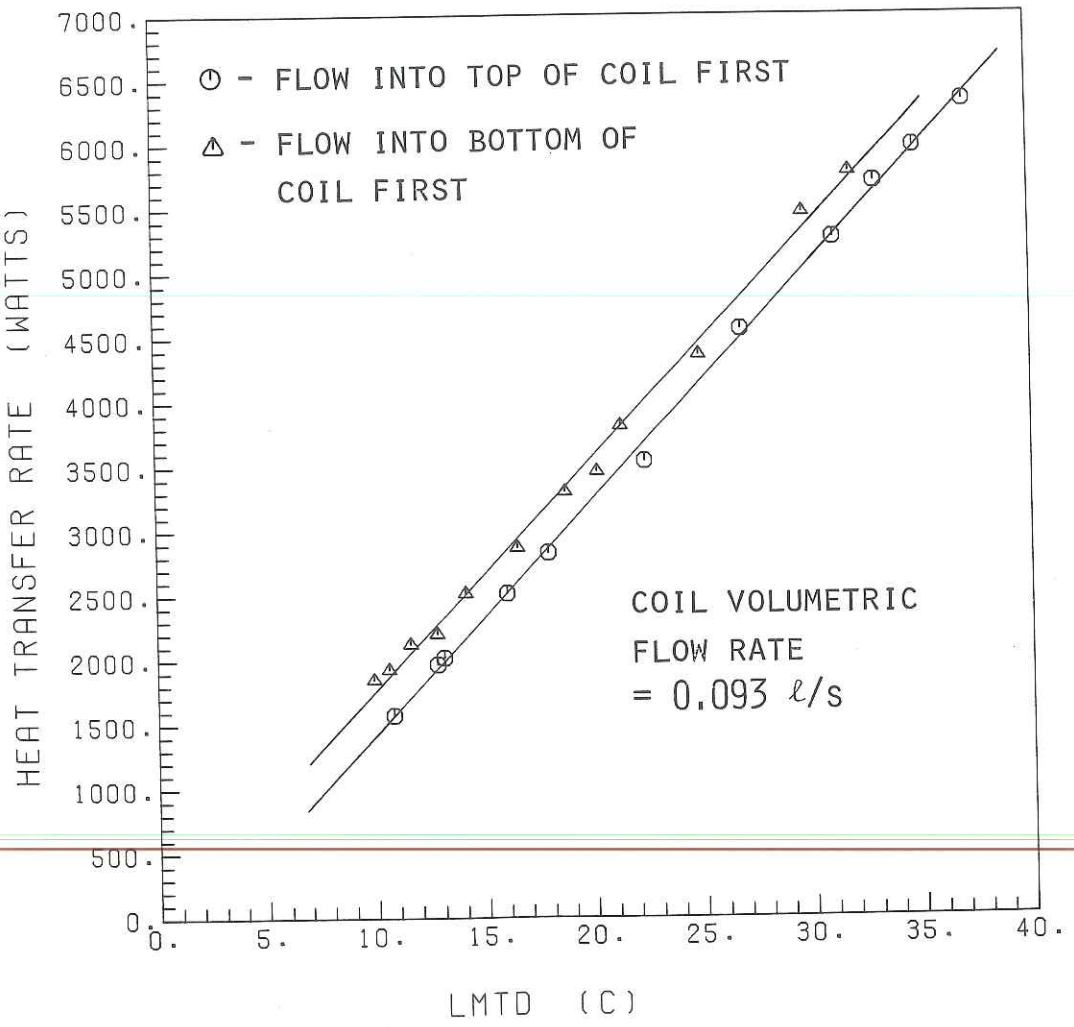

Figure 5.2.1 A comparison of coil performance between water into the top of the coil first and water into the bottom of the coil first

The reason for this behavior is not known. A possible reason may be a combination of hydrodynamic and thermal interaction effects which are discussed in the Discussion and Conclusions Chapter.

5.3 Parallel Immersed Coil Flow Versus Series Flow

Two multi-pass, smooth-tube, immersed coils were mounted in the side of the storage tank as described in Chapter 2. When not considering the direction of the flow through the coils, there are essentially two ways to connect the coils to the hot water source tank. The first way is to connect the immersed coils in series so the hot source water flows through one coil then the other. The second way is to divide the flow in half to enter each coil separately and simultaneously thus creating a parallel flow arrangement. The measured heat-transfer rate from the series coil is,

$$q_s = \dot{m}\, C_p\, (T_{c,i} - T_{c,o})_{1,2} \qquad 5.3.1$$

where $T_{c,i}$ is the temperature of the water entering the coils and $T_{c,o}$ is the temperature of the water leaving the coils. Subscripts 1 and 2 represent the two coils. The measured heat-transfer rate from the parallel arrangement is:

$$q_p = \frac{\dot{m}}{2}\, C_p\, (T_{c,i} - T_{c,o})_1 + \frac{\dot{m}}{2}\, C_p\, (T_{c,i} - T_{c,o})_2 \qquad 5.3.2$$

For the parallel flow configuration, the temperature of the water from the source tank was measured and then it was divided into two equal flows to enter each coil. The temperature of the water leaving each coil was measured separately. The length and configuration of each side of the parallel flow arrangement were identical to assure equal flow.

The experiments conducted compared the performance of the parallel configuration to that of the series arrangement. All tests involved storage tank heating with no load draw. The initial storage tank temperature was about 10.°C to 15.°C and the final tank temperatures ranged from 65.°C - 70.°C. Coil volumetric flow rates tested were from 0.063 ℓ/s to 0.125 ℓ/s (before dividing the flow in the parallel case).

Results:

The series flow configuration is superior to the parallel flow configuration as can be seen in Figure 5.3.1. In the temperature range tested, the series coil performs roughly 20%-25% better than the parallel coil configuration. One obvious reason for part of this behavior is that the volumetric flow rate (and velocity) of the water through each immersed coil with the parallel configuration is half that of the series configuration. This reduces the convection coefficient, h, at the interior surface of the coil and thus reduces the overall heat-transfer coefficient-area product, UA of

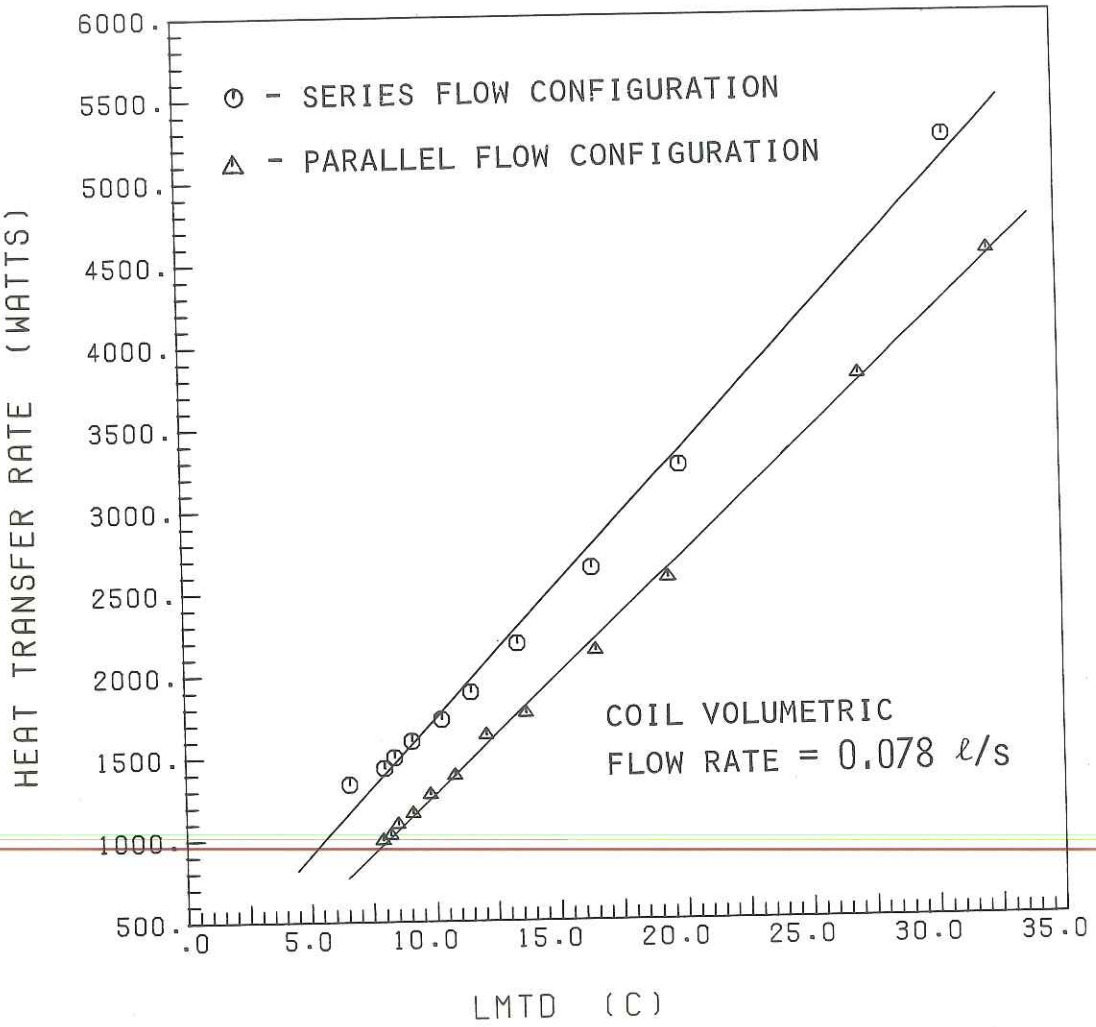

Figure 5.3.1 A comparison of series and parallel flow configurations

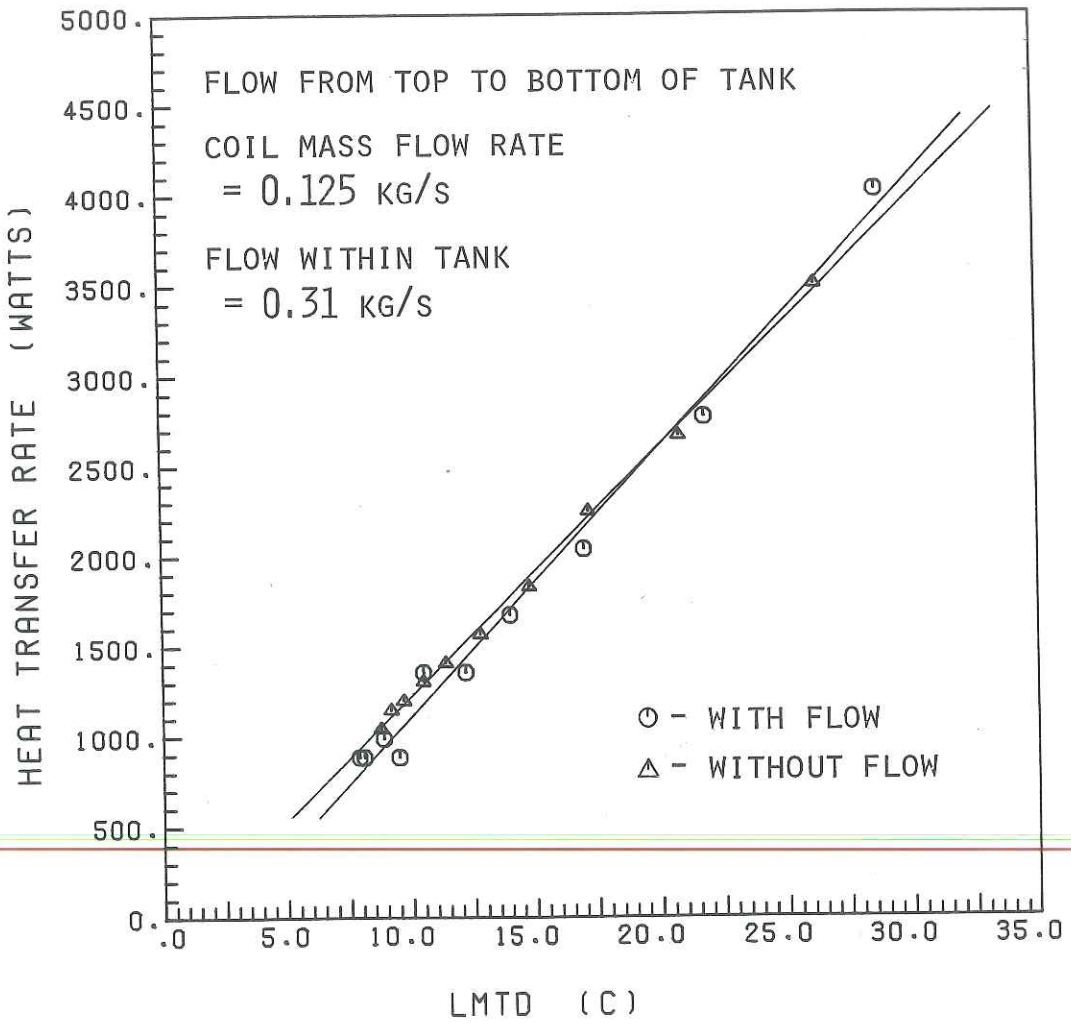

Figure 5.4.1 Exterior coil flow comparison

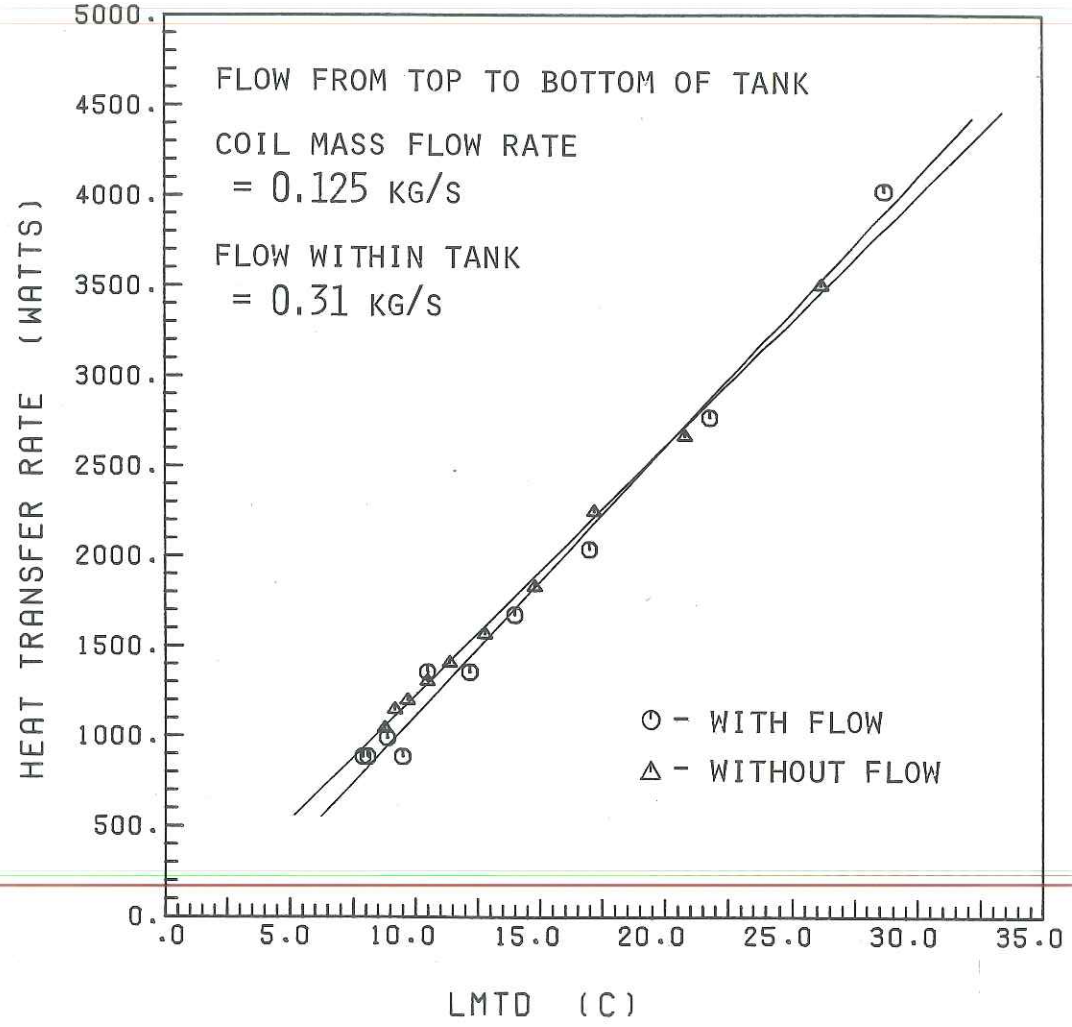

Figure 5.4.1 Exterior coil flow comparison

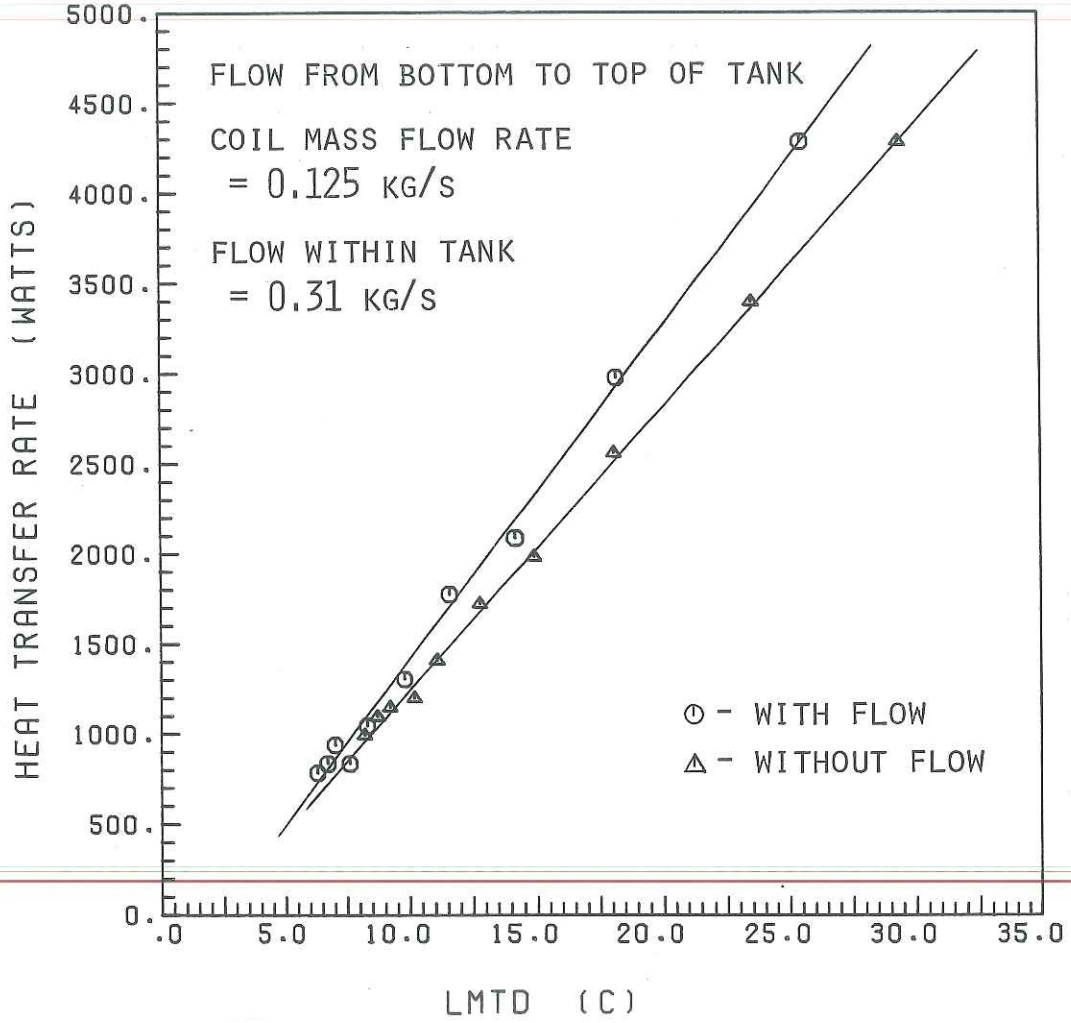

Figure 5.4.1 Exterior coil flow comparison
(continued)

performance when there is tank flow. The slight flow due to the movement of water in the storage tank enhances the free-convection currents surrounding the immersed coil since both flows are in the upward direction. For the condition of storage tank flow in the upward direction, the measured value of the convection heat-transfer coefficient, h, increased approximately 30% over the no-flow condition.

5.4.2 Exterior Immersed Coil Flow Utilizing a Nozzle

Carrying the idea of external flow over an immersed coil one step further, the nozzle of Figure 5.4.2 was constructed. The longitudinally cut slits produced a fan-like spray which covers an area of nearly the size of the multi-pass, smooth-tube coil. With this nozzle design and a pumping rate of 0.30 ℓ/s (pump limit), the velocity of the water at the nozzle exit was 0.90 m/s. The nozzle was placed 0.10 m beneath the multi-pass, smooth-tube coil (2 coils, one situated above the other) to create one upwards flow (see Figure 5.4.3). Water was drawn off the bottom of the tank, below the level of the coils and pumped back in through an opening in the top of the tank, down a tube to the nozzle. All piping outside of the storage tank was well insulated to minimize thermal losses. The velocity of the water past the coils was not obtainable except that it was somewhere below 0.90 m/s (the velocity at the nozzle exit). Again, a series of storage tank heating tests were run with initial tank temperatures at around 10.°C to 15.°C and final tank

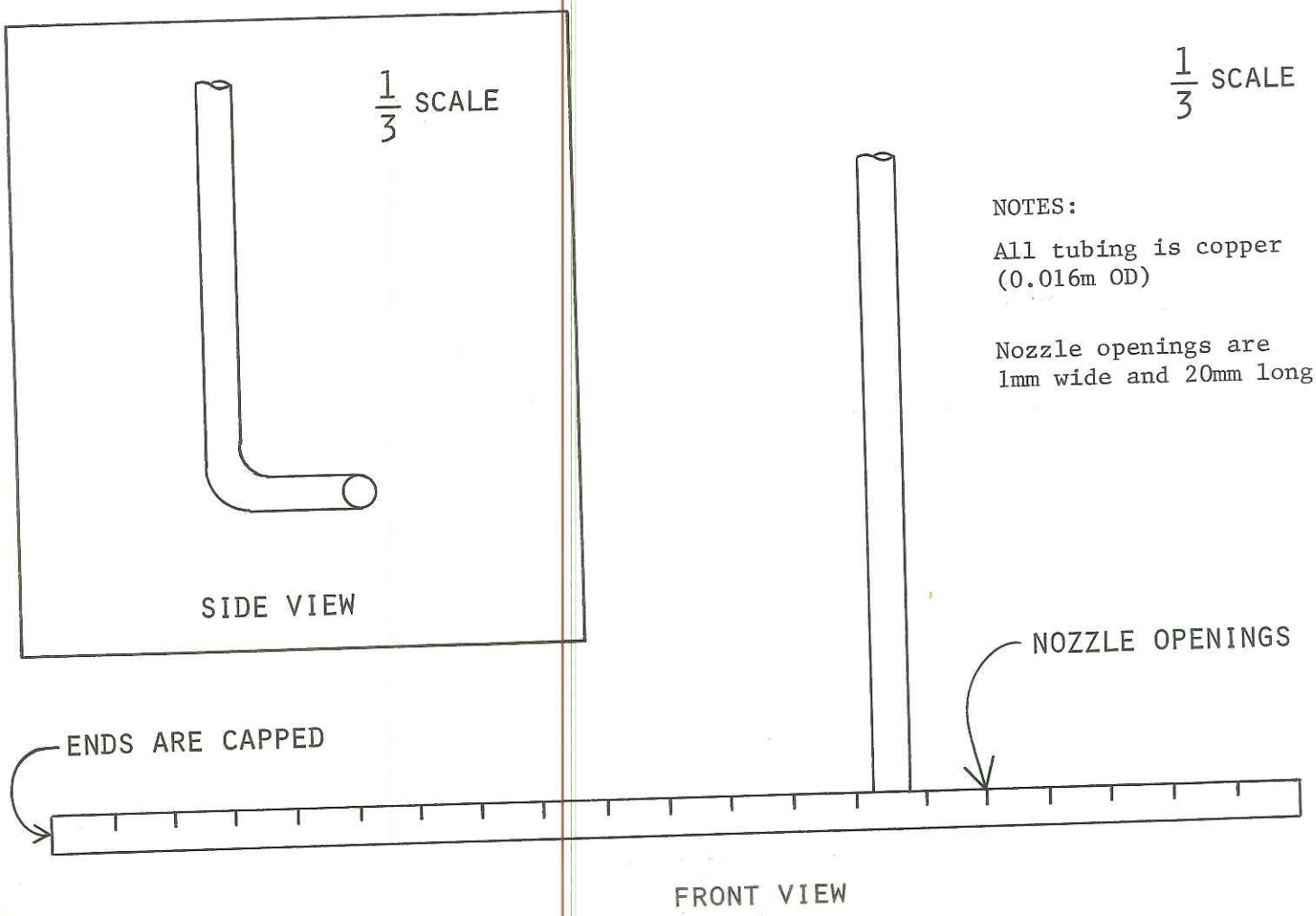

Figure 5.4.2 Nozzle diagram

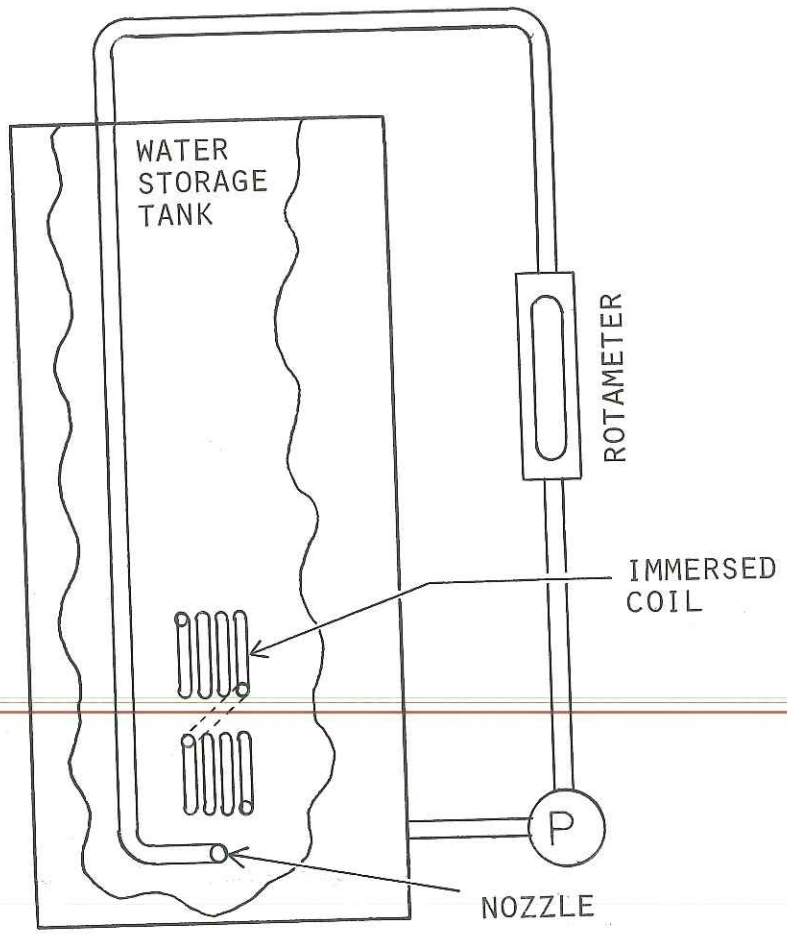

Figure 5.4.3 Storage tank with nozzle installed

temperatures (10-12 hours later) of 65.°C to 70.°C. Two coil volumetric flow rates; 0.093 ℓ/s and 0.125 ℓ/s were tested. Comparisons were made between tests with the nozzle operating and tests with the nozzle turned off.

Results:

Figure 5.4.4 shows dramatic increases in immersed coil performance when utilizing the nozzle. The average velocity of the water across the exterior of the immersed coil is significantly increased. The overall heat-transfer coefficient-area product is increased by about 50%. This implies that for a given log-mean temperature difference, the heat-transfer rate is about 50% greater for the immersed coil while using the nozzle than without the nozzle. The effect of using the nozzle with the immersed coil on other coil parameters is as equally dramatic. Coil effectiveness, ε, increases by about 40% and the average convection coefficient, h, for the exterior of the coil increases by up to 400%. This reduces the external thermal resistance to the same order of that for the internal resistance. The major resistance to heat transfer for this coil now is that due to the contact resistance between the two tubes of the wall in the double-wall coil. Any significant improvement in coil performance must now come from a reduced coil wall thermal resistance.

There are several disadvantages to this idea. First, addi-

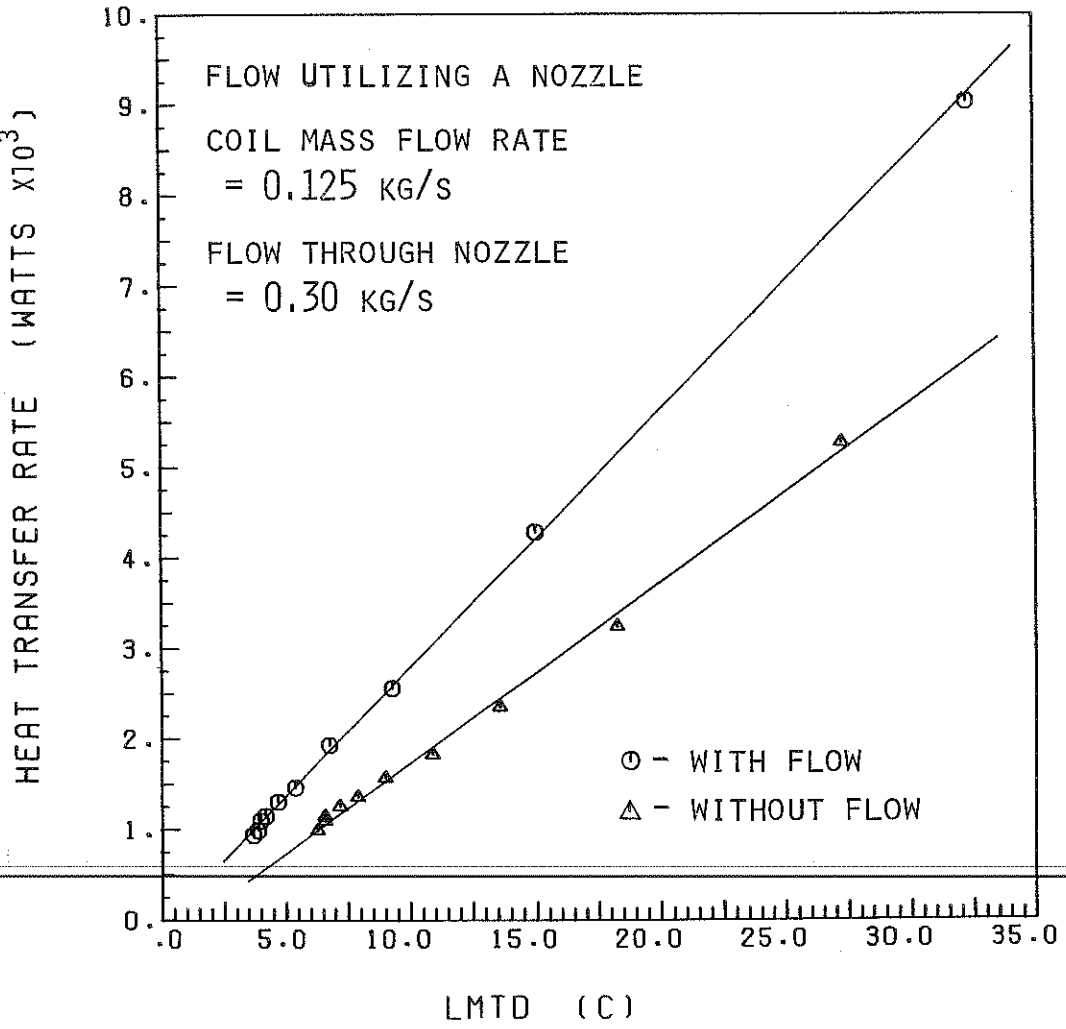

Figure 5.4.4 Exterior coil flow comparison
(utilizing a nozzle)

tional parasitic power is required to operate the pump. Second, additional plumbing is needed and third the nozzle openings tend to plug up with mineral deposits when using unsoftened water. The use of a nozzle in a water storage tank would probably be more cost effective in larger, industrial applications. In larger systems the cost of the additional equipment would be a smaller percentage of the overall system cost and the savings would be more dramatic.

5.5 Tailoring the Free Convection Flow

In section 5.4 the method of increasing immersed coil performance by producing a forced convection heat transfer condition on the exterior of the coil was discussed. A major disadvantage was that it required an extra pump and extra parasitic power to move the water. In this section a discussion of an experiment designed to tailor the flow of free convection currents to increase coil performance is discussed.

Situated below the immersed coil is a layer of water that is only minimally affected by the coil. Its temperature is lower than that of the rest of the tank. A chimney was constructed of plastic sheet and positioned within the storage tank as shown in Figure 5.5.1. This chimney is 0.8 m long and has a 0.09 m diameter. Holes were cut in the side to allow insulated leads to connect to the coil. The bottom of the chimney rests on the bottom of the storage tank and has holes cut in the side to allow the cool water to enter--the top is open.

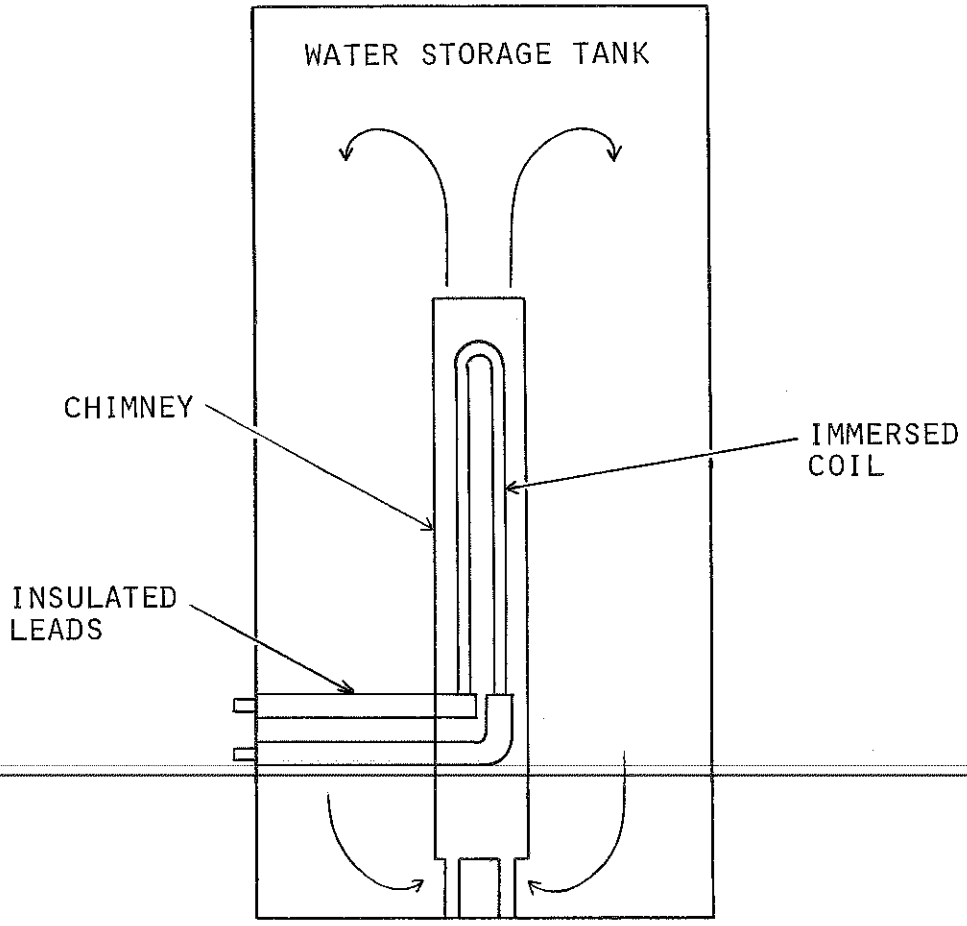

Figure 5.5.1 Storage tank with chimney installed around coil

The coil inside the chimney is a single-pass, smooth-tube coil with a surface area of 0.057 m^2 (shown in Figure 2.1.2c). It is mounted vertically within the chimney (due to space and access limitations) with the bottom of the coil located 0.25 m from the bottom of the tank. The water in the vicinity of the coil is heated by the coil and then rises to exit out the top of the chimney. This action draws cool water into the chimney through the holes cut in the bottom. A continuous flow is thus set up through the chimney, past the immersed coil. Ideally the free convection flow set up by this arrangement is significantly greater than if there were no chimney.

The tests with the chimney were all storage tank heating tests (there was no load draw). The storage tank temperature was initially 10.°C to 15.°C. After heating, the tank temperatures were generally 50.°C to 55.°C. The coil volumetric flow rates tested were from 0.075 ℓ/s to 0.125 ℓ/s. Comparisons were made between the immersed coil with the chimney surrounding it and with the chimney removed.

Results:

By referring to Figure 5.5.2, we can see that the performance of the immersed coil is 15%-20% better <u>without</u> the chimney in place than with it in place. At a coil volumetric flow rate of 0.10 ℓ/s, the average overall heat-transfer coefficient-area product, UA, for the immersed coil with the chimney in place was 37.0 W/°C. When the chimney was not in place the average UA was 44.2 W/°C. Similar re-

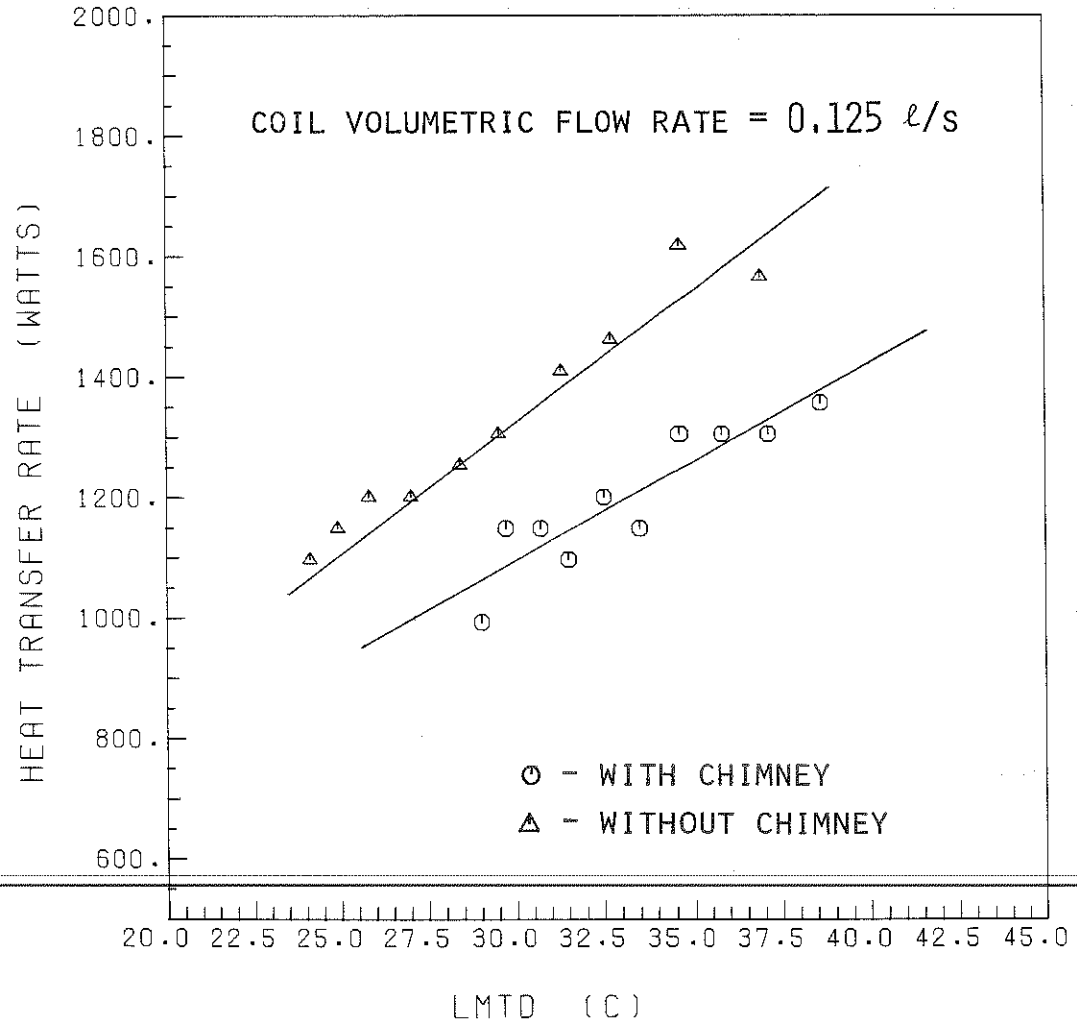

Figure 5.5.2 A comparison of the single-pass coil with and without the chimney

sults were observed for all coil volumetric flow rates tested. This particular chimney design actually inhibits coil performance. Possible reasons for this are:

1) The size of the openings at the bottom of the chimney may be inadequate. The small openings may be constricting flow into the chimney.
2) The diameter of the chimney may not be optimal. A visual inspection (with dye injected) of the coil and chimney in operation showed that the water of the storage tank was entering around the edge of the top opening of the chimney and exiting at the center of the top opening.
3) The chimney may be interferring with an overall natural convection flow within the tank which may have a greater effect on the heat transfer of the coil than any effect a chimney would have.

Further investigation into this idea is needed before definite conclusions can be drawn about the value of tailoring the free-convection flow to enhance coil performance through the use of something like the described chimney.

5.6 Immersed Coil Orientation

Based on empirical equations [9], a horizontally oriented cylinder has better heat transfer characteristics than a vertically oriented one. It may be a safe assumption to carry this over into

immersed heat exchanger coils--a horizontally orientated coil is more effective than a vertically orientated one for a given temperature difference. However, there are other factors involved with heat exchanger coils. The close proximity of the storage tank wall may have some effect on the convective flow patterns around the coil. Also, immersed coils are generally not simple horizontal, straight tubes. The next section describes a series of experiments designed to determine the effect of coil orientation on coil performance.

5.6.1 Orientation Experiment

A single-pass, smooth-tube coil heat exchanger (shown in Figure 2.1.2c) was mounted in the storage tank with one end located 0.4 meters above the bottom of the tank. Three orientations were tested. The first coil orientation was horizontal, (0° inclination), the second was mounted with an incline of 45° from horizontal and the third orientation was vertical (90° inclination). Both the 0° inclination and 45° inclination coils were mounted to the side of the tank. The 90° inclined coil was mounted in the center of the storage tank with insulated leads to connect it to the side. All three coil orientations have an exposed coil surface area of $0.057\ m^2$.

Storage tank heating experiments were conducted with no load draw. Each orientation was tested at three coil volumetric flow rates; 0.075 ℓ/s, 0.10 ℓ/s and 0.125 ℓ/s. The initial storage tank

temperature was about 10.°C - 15.°C and final tank temperatures were about 50.°C - 55.°C. Each test required about 12 hours to heat the storage tank.

Results:

Figure 5.6.1 shows the results of the orientation experiments. As one might expect, the horizontal immersed coil is superior. Beyond that, it is unclear whether the 45° or 90° coil orientation is better in the temperature range tested. Similar results were found for the other coil flow rates tested. The close proximity of the storage tank wall appears to have no effect on the expected performance of the coils relative to one another. Reasons for the difference in immersed coil performance due to orientation may be caused by boundary layer thickness. The convective currents from the vertical coil rise along the coil. As the currents rise, the boundary layer becomes thicker causing greater thermal resistance. For the horizontal coil, the convective currents rise away from the coil--thus keeping the boundary layer thickness to a minimum. The coil orientation of 45° should perform somewhere between these two extremes. From the data, the performance of the 45° orientated coil is much closer to the performance of the vertical coil than that of the horizontal one.

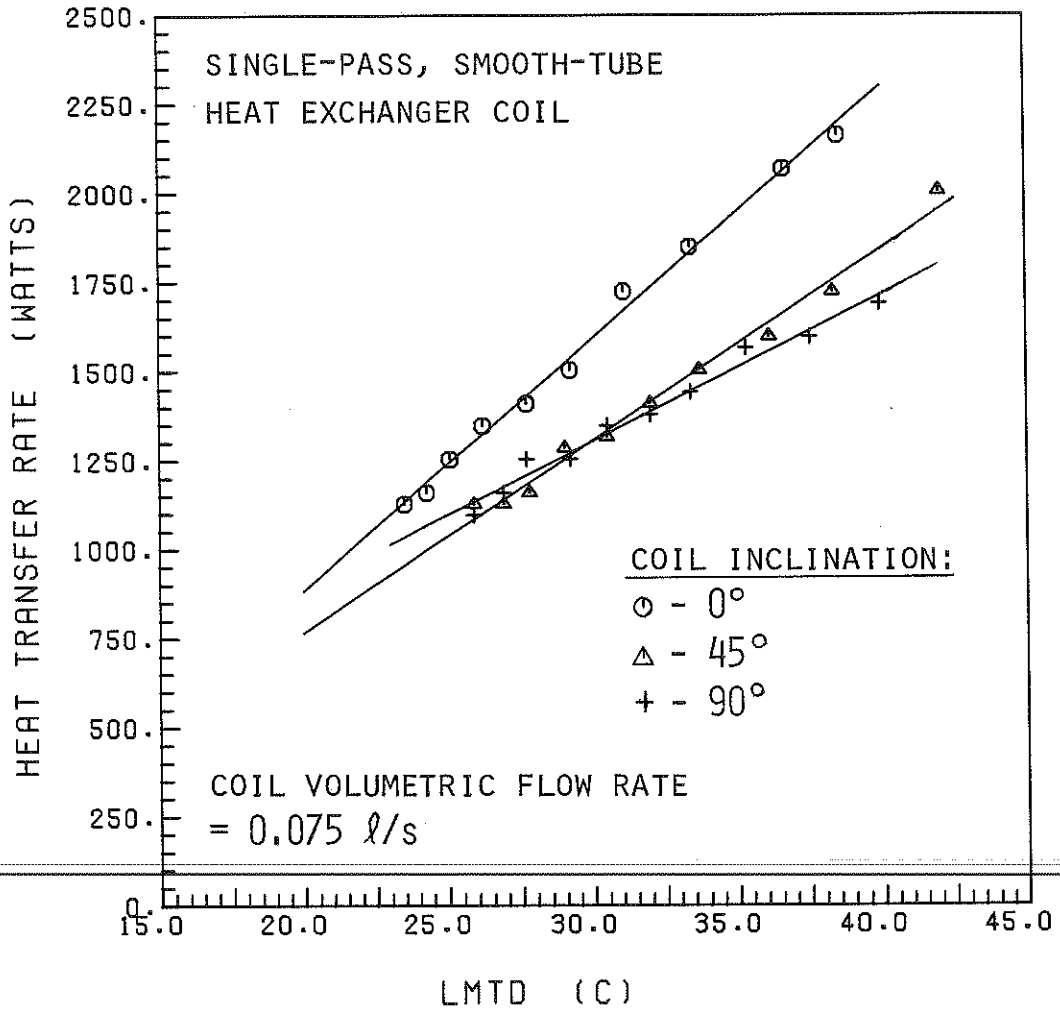

Figure 5.6.1 Results of the immersed coil inclination experiments

6.0 Computer Simulation

The purpose of this chapter is to show that the performance of a storage tank with an immersed coil heat exchanger can be accurately simulated on a computer with simple models. The simulation program used was TRNSYS [2]. Several assumptions are made such as; constant coil effectiveness, fully mixed tank and the heat exchanger type. These assumptions are explained and justified in the following sections. Two simulations were run; storage tank heating with and without a load draw. The results are compared to experimental data.

6.1 Assumptions

6.1.1 Fully Mixed Storage Tank

The simplest TRNSYS model assumes a one-node, fully mixed tank. This is a fairly accurate assumption when there is no load draw on the storage tank. When using a common type of coil such as the multi-pass, smooth-tube coil (2 coils, one mounted above the other) it was noted that the variation in temperature from the top of the tank down to the level of the coil was about 0.5°C. The temperature of the water below the coil typically varied no more than 1.0°C or 2.0°C from that above the coil. The volume of water located below the coil is only about 5% of the total volume of water in the storage tank so it has little effect on the variation in bulk storage tank

temperature. The variation of 0.5°C is on the same order as the accuracy of the temperature measurements. Therefore one temperature can be measured to be that of the entire tank (down to the accuracy of the temperature measuring instruments).

When a load draw is applied to the storage tank, there is significant stratification within the tank (see Figure 6.1.1). Stratification of the storage tank disappears very soon after the load draw ceases. In the following TRNSYS simulations, the existance of stratification is ignored. This may be the cause of some inaccuracies in the simulation since the assumption of constant effectiveness (discussed in the next section) is least accurate during periods of storage tank stratification.

6.1.2 Constant Coil Effectiveness

Coil effectiveness is found to be nearly independent of the temperature difference. Figure 6.1.2 shows coil effectiveness as a function of temperature difference between the coil inlet and the tank for the horizontal, multi-pass, smooth-tube coil (2 coils, one mounted above the other). As expected, there is a definite trend towards increasing effectiveness with increasing temperature difference. However, an average value of 0.33 represents the effectiveness of this particular coil at a flow rate of 0.10 ℓ/s to within 0.04. This is typical of the variation in effectiveness with the temperature differences obtained for the four coil configurations tested. A value for coil effectiveness can be found through the method des-

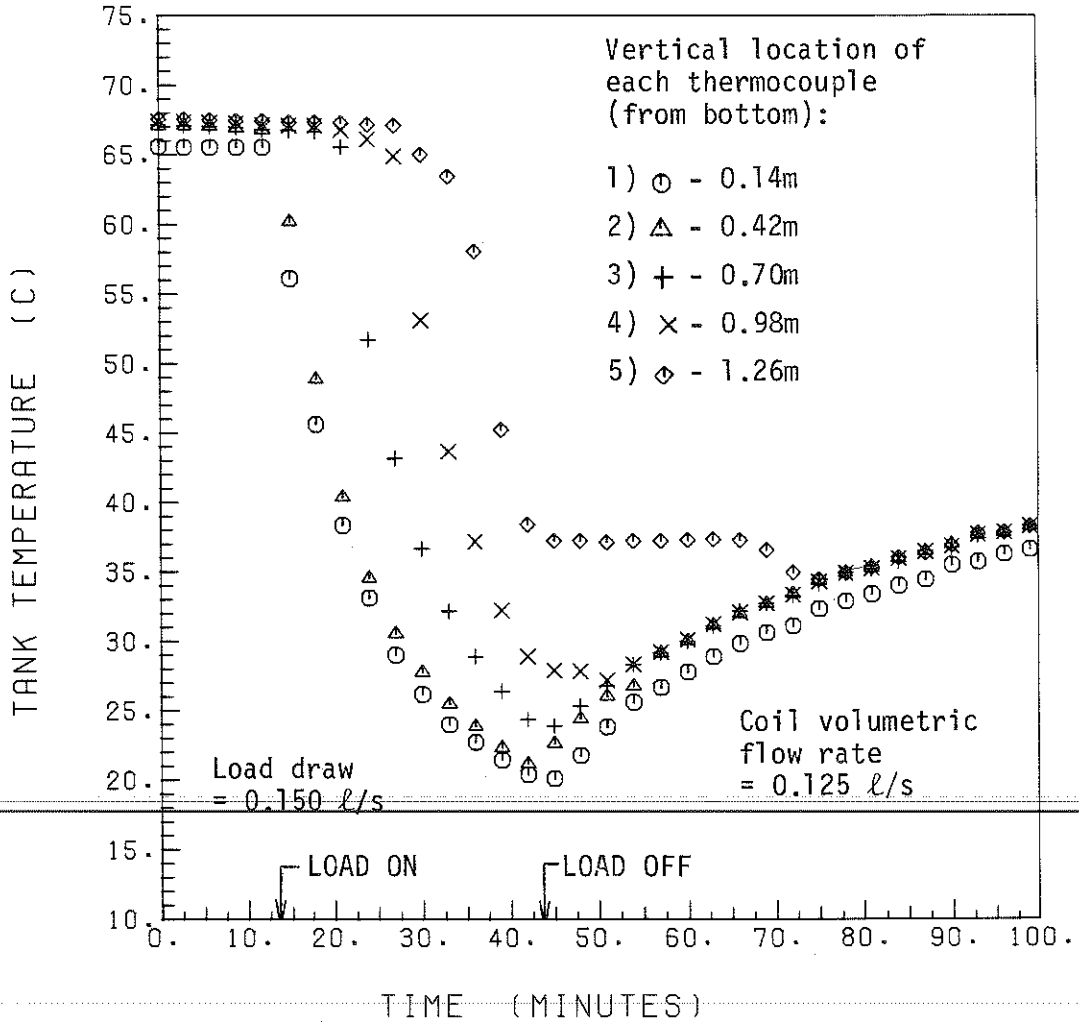

Figure 6.1.1 An example of storage tank stratification during a load draw

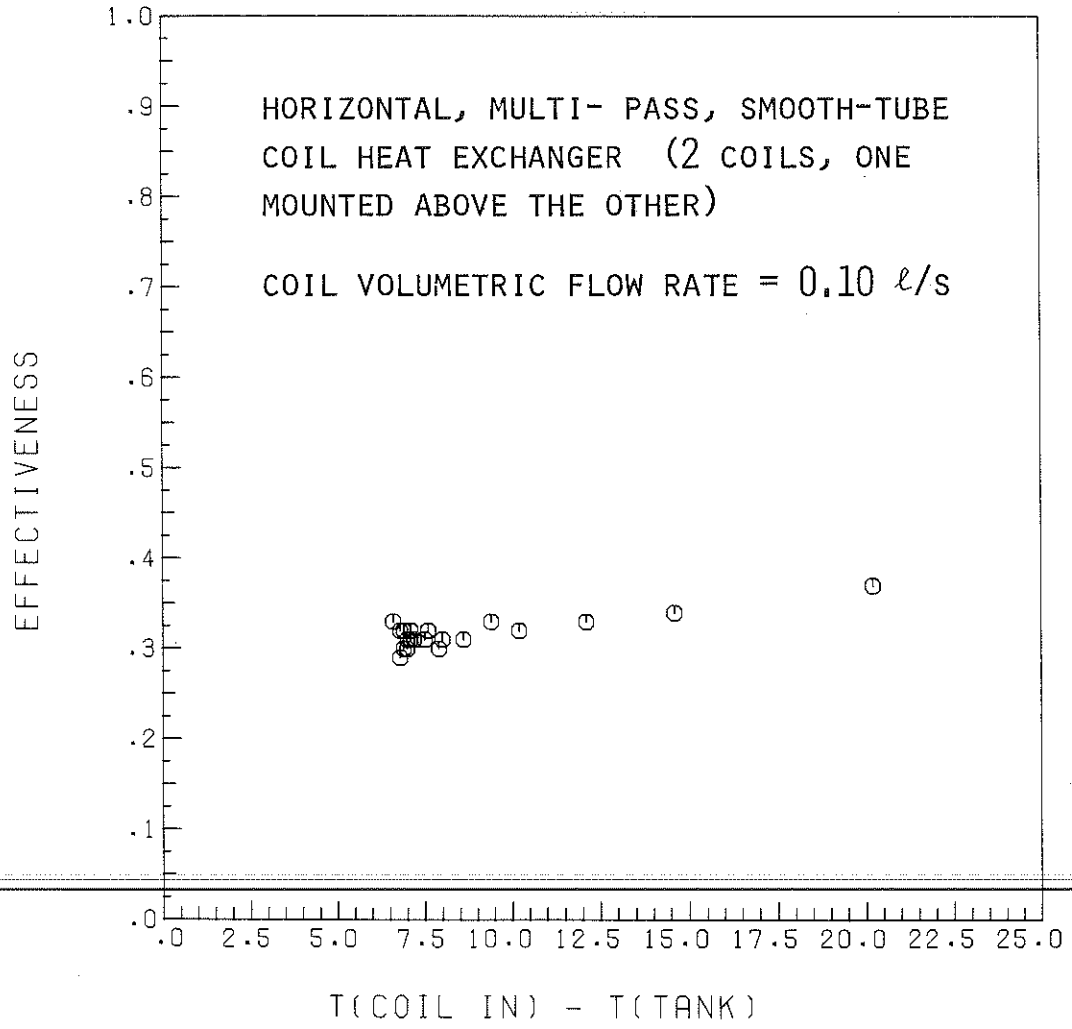

Figure 6.1.2 An example of nearly constant coil effectiveness

cribed in the sample problem of Appendix B or through experimentation.

6.1.3 Heat Exchanger

TRNSYS does not have provisions to directly model the internal heat exchanger coil, (natural convection on the cold side and forced convection on the hot side). An external, zero capacitance, sensible heat exchanger model with a constant effectiveness can be used to simulate the internal heat exchanger coil. This exchanger assumes forced flow on both the hot and cold sides. The value of the exchanger fluid mass flows for both sides is set equal to the immersed coil mass flow rate. The maximum possible heat transfer is calculated based on the minimum capacity rate fluid and the cold side and hot side fluid inlet temperatures. The minimum capacity rate fluid is the hot side since the cold side (the storage tank) must be considered to have infinite capacity due to the fact that the temperature of the water on the exterior side of the coil (T_T) in constant along its length. When referring to Figure 6.1.3 (description of the modeled heat exchanger) we see that $\dot{m}_c$ is set equal to $\dot{m}_h$ and $T_{c,i} = T_{c,o}$ (due to a fully mixed tank in reality). Therefore the minimum capacity rate fluid is:

$$C_{min} = (C_p \dot{m})_h = C_h \qquad 6.1.1$$

where $C_{p,h}$ is the specific heat of water and $\dot{m}_h$ is the mass flow

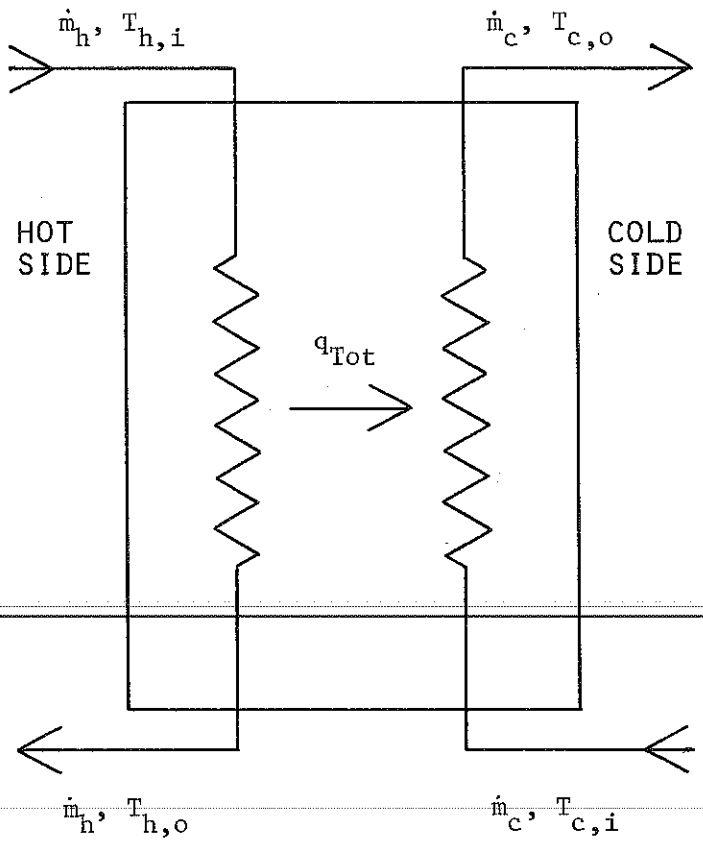

$C_c = \dot{m}_c C_{p,c}$

$C_h = \dot{m}_h C_{p,h}$

Set:

$\dot{m}_c = \dot{m}_h$

$T_{c,i} = T_{c,o}$

$C_{min} = C_h$

Use a constant value for heat exchanger effectiveness, ε.

Figure 6.1.3 TRNSYS model heat exchanger

rate of the water through the coil. The maximum possible heat transfer is:

$$q_{max} = C_h (T_{h,i} - T_T) \qquad 6.1.2$$

The total rate of heat transfer becomes,

$$q_{Tot} = \varepsilon\, q_{max} \qquad 6.1.3$$

therefore,

$$T_{h,o} = T_{h,i} - \frac{q_{Tot}}{C_h} \qquad \text{and} \qquad 6.1.4$$

$$T_{c,o} = T_{c,i} + \frac{q_{Tot}}{C_c}$$

where C_c is infinite.

6.2 Overall Tank-Loss Coefficient, U, Calculation

One of the parameters required as input for the TRNSYS Fluid Storage Tank component is a value for the overall tank-loss coefficient, U, of the storage tank. The following shows how U is calculated from measured data.

The overall loss coefficient was calculated with a lumped-capacity cooling model [9]. An energy balance on the tank yields:

$$\frac{dT}{dt} = \frac{-UA}{mC_p} (T - T_\infty) \qquad 6.2.1$$

With initial conditions of $T = T_o$, the initial temperature of the tank and $t = 0.$ at time zero. The solution is,

$$\ell n \frac{T - T_\infty}{T_o - T_\infty} = - \frac{UA}{mC_p} t \qquad 6.2.2$$

With equation 6.2.2, it is necessary only to measure the tank bulk temperature as a function of time and the environment temperature to obtain $-UA/mC_p$. When $\ell n \frac{T - T_\infty}{T_o - T_\infty}$ is plotted as a function of time, the slope of the resulting line is $-UA/mC_p$. Knowing the physical parameters of the storage tank* and water, we can obtain a value of the overall loss coefficient of,

$$U = \frac{- (\text{slope}) \times m_w \times C_p}{A_T} \qquad 6.2.3$$

where: m_w = the mass of the water in the thermal storage tank.

C_p = the specific heat of water.

A_T = the outside area of the water storage tank case exposed to the environment minus the bottom area since it is well insulated (in this case).

A plot of $\ell n \frac{T - T_\infty}{T_o - T_\infty}$ as a function of time is shown in Figure 6.2.1. This plot is the result of a cooling experiment conducted

*The storage tank physical properties are listed in Appendix A.

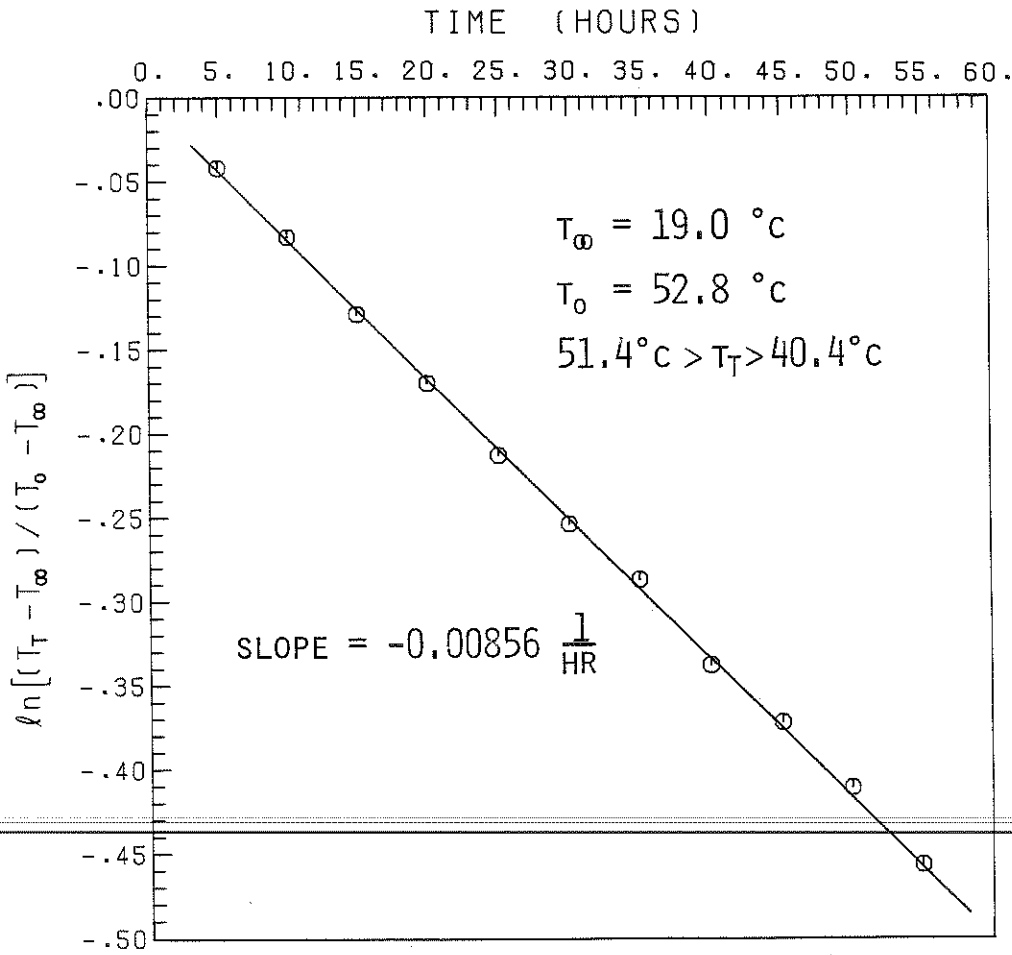

Figure 6.2.1 Results of the storage tank cooling experiment

on the water storage tank used in all experiments. The cooling experiment was conducted over a period of 55 hours with the initial tank temperature being 53.°C and the final tank temperature being 40.°C. The ambient temperature averaged 19.3°C. The slope of the resulting line is $-0.00856 \frac{1}{hr}$. Using equation 6.2.3 we get,

$$U = \frac{-(\text{slope}) \times (m_w) \times (C_p)}{A_T} = \frac{-(-0.00856 \frac{1}{hr}) \times (333.\ kg) \times (4179. \frac{J}{kg°C})}{(3.70\ m^2)\ (3600 \frac{s}{hr})}$$

$$U = 0.89 \frac{W}{m^2 °C}$$

6.3 Experimental Procedure to Obtain Temperature Data for a Comparison with TRNSYS Simulation

Initially storage tank heating with no load was simulated. The storage tank was filled with main water at about 15.°C. Various coil volumetric flow rates (0.075 ℓ/s to 0.125 ℓ/s) with no load draw from the storage tank were tested. The storage tank was heated up over a period of 12 hours to a temperature in the 60.°C - 70.°C range. The tank temperature, the temperature of the water entering and leaving the coil and the environment temperature were monitored over the duration.

Inputs to TRNSYS for the simulation of storage tank heating with no load were the temperature and volumetric flow rate of the water entering the immersed coil, the environment temperature and

the value of coil effectiveness. Outputs are the storage tank temperature and the immersed coil outlet temperature.

Further experiments were conducted which added a load draw to the storage tank and this was also simulated. The volumetric flow rates of the load draw were chosen to simulate residential usage of hot water. The rates varied from 0.075 ℓ/s to 0.15 ℓ/s. To simplify the comparisons, the load draws lasted for half-hour periods.

Inputs to TRNSYS for the simulation of the load draw experiments were the same as for the storage tank heating with no load simulation plus additional inputs of the volumetric flow rate and the temperature of the storage tank replacement water.

6.4 Results and Comparisons

The output of the computer simulation is compared to the experimentally measured data for the storage tank heating in Figure 6.4.1. This comparison had an immersed coil volumetric flow rate of 0.10 ℓ/s, an environment temperature of 19.8°C and immersed coil inlet temperatures varying from 70.2°C to 51.8°C. The experimentally measured storage tank temperatures agree with the computer simulation storage tank temperatures to within 1.°C over the entire period of the simulation. The storage tank temperature initially increases quite rapidly due to the large temperature difference between the immersed coil average temperature and the storage tank temperature.

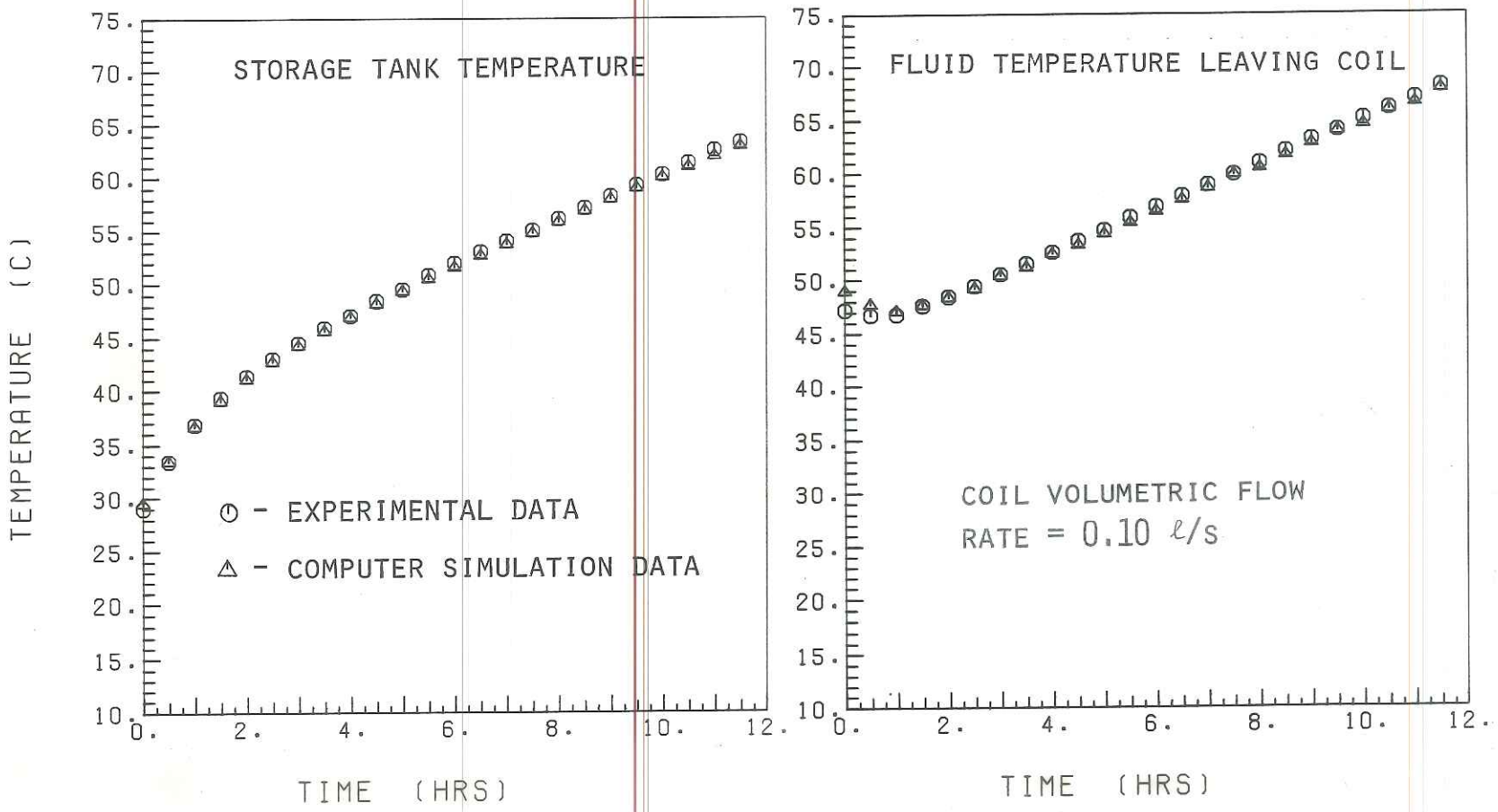

Figure 6.4.1 A comparison of the TRNSYS computer simulation with experimental data (without storage tank load)

The rate of tank temperature increase slows and becomes nearly linear from about hour 4 to hour 12. During this time, the coil inlet temperature increases along with the storage tank temperature. Although the plot does not show a temperature profile beyond 12 hours, the temperature approaches 72.°C (the source tank set temperature).

The comparison between the measured data and the computer simulation data of the coil outlet temperature (also shown in Figure 6.4.1) also shows agreement to within 1.°C except during the first three time steps. The reason for this inaccuracy results from using an average constant value for coil effectiveness. This assumption is least accurate at the beginning of a heating experiment when the difference between the average coil temperature and the storage tank temperature is greatest. As seen in Figure 6.4.2, the value of coil effectiveness at the beginning of the storage tank heating experiment used for comparison, is actually greater than the overall average effectiveness.

Figure 6.4.3 shows the comparison between the experimentally measured data and the computer simulation output for a load draw situation. The agreement is reasonable; an 18 hour simulation of the storage tank temperature produces a final tank temperature that agrees with the measured temperature again to within 1.°C. The initial load draw was 0.15 ℓ/s at hour 1. The second load draw was 0.075 ℓ/s at hour 7 and the third load draw was 0.10 ℓ/s at hour 13. Each load draw lasted one-half hour. The temperature of the replace-

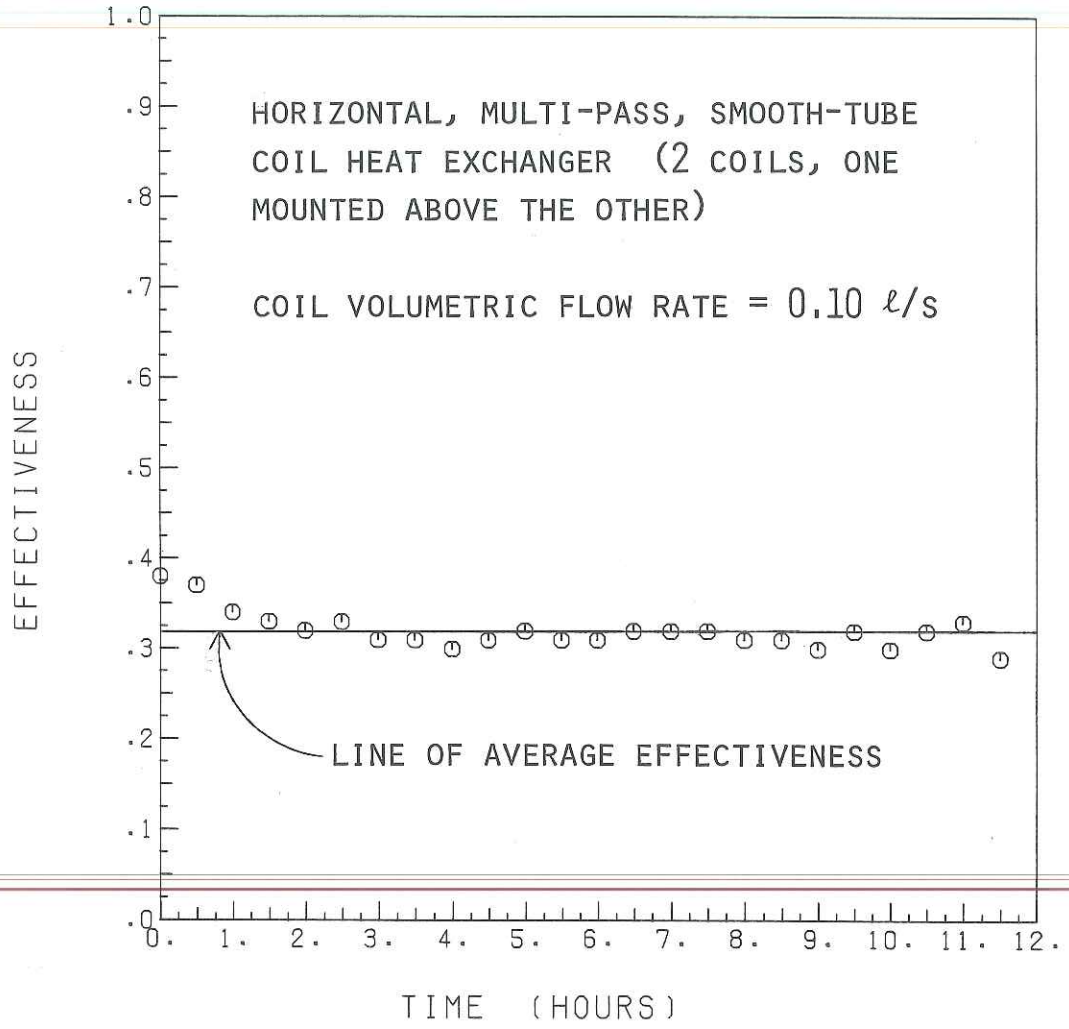

Figure 6.4.2 Coil effectiveness as a function of time

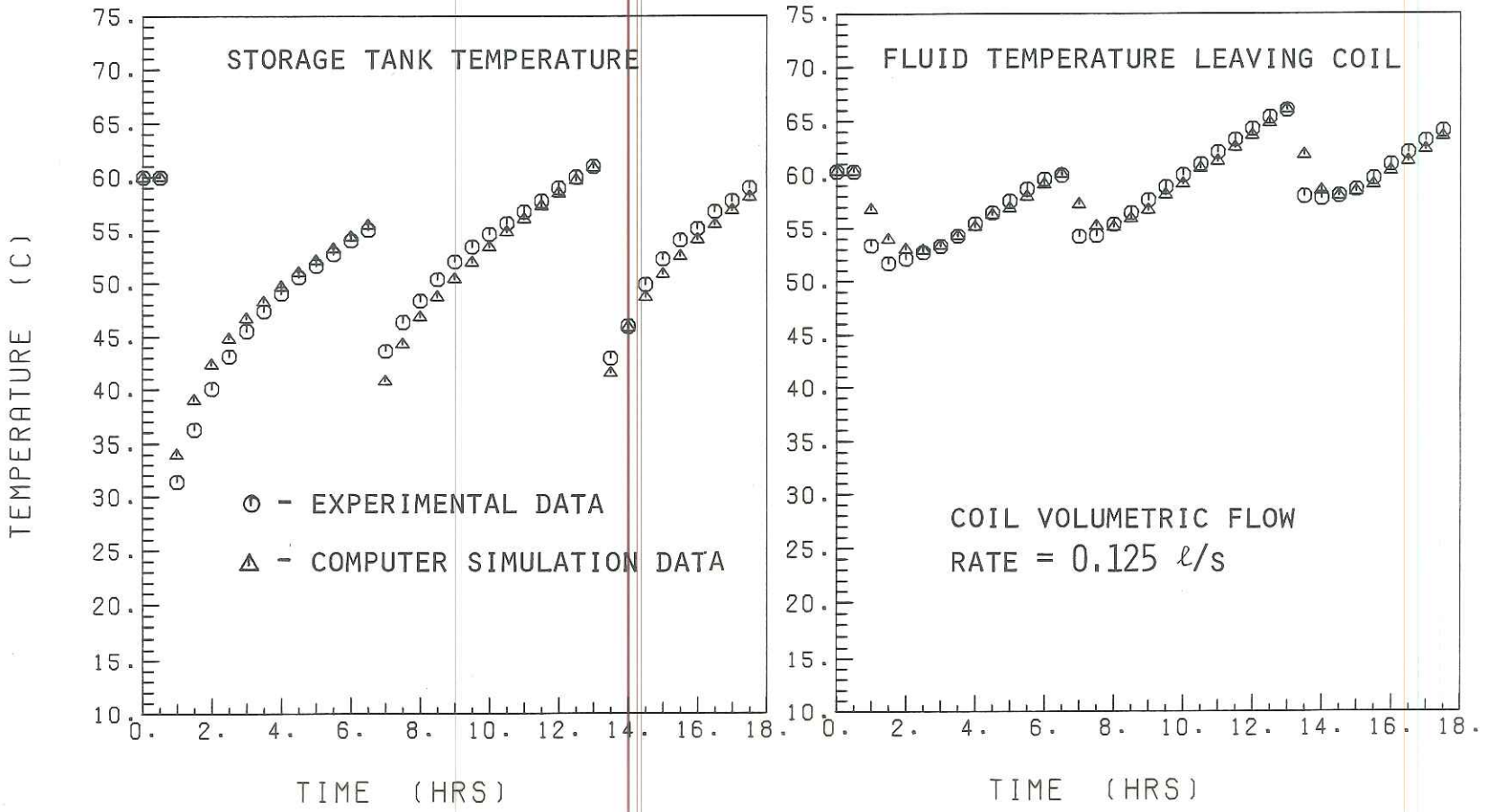

Figure 6.4.3 A comparison of the TRNSYS computer simulation with experimental data (with a storage tank load)

ment water from the main was between 10.°C and 15.°C for all three loads. The areas of poorest agreement occur immediately after the load draws cease. At these points, the difference between the average coil temperature and the storage tank temperature is greatest and again the instantaneous value of effectiveness at these points is significantly greater than the overall average effectiveness of the coil.

Looking at the comparison of experimental and measured values of the coil exit temperature, we can see close agreement except immediately after a load draw. The reason for this discrepancy is the same as stated above for the tank temperature discrepancies.

The TRNSYS decks used in the two preceding simulations are listed in Appendix D.

7.0 Discussion and Conclusions

Very minimal temperature stratification is observed in the thermal storage tank above the location of the heat exchanger coil when there is no load draw on the tank. This finding is in agreement with experimental results obtained elsewhere [4]. Apparently, the convection currents produced by the heat exchange process are sufficient to thoroughly mix the water at all points above the immersed coil. Stratification is observed while there is a load draw placed on the water storage tank but soon disappears shortly after the load ceases. Figure 6.1.1 is a plot of the tank temperature distribution as a function of time for a load draw. The immersed coil volumetric flow rate is 0.125 ℓ/s and the load draw is 0.15 ℓ/s for one-half hour. At the end of the half hour load draw, the variation in storage tank temperature is from 21.°C at the level of the immersed coil to 38°C at the top of the tank. The lowest temperature measurement is taken below the level of the immersed coil at the bottom of the tank which is minimally affected by the convection currents. Essentially all temperature stratification above the level of the coil disappears within one-half hour after the load draw ceases.

Immersed coil effectiveness is found to be nearly independent of the temperature difference between the coil inlet and the tank. Figure 6.1.2 shows this relationship for two horizontal, multi-pass, smooth-tube coils (shown in Figure 2.1.2a) connected in series and

mounted one above the other. The trend shows a definite increase in effectiveness as the temperature difference increases. However, an average value of 0.33 represents the effectiveness of this particular coil arrangement to within 0.04. This is typical of the variation in effectiveness with the temperature difference for the four immersed coil configurations tested. The ability to assume a constant effectiveness greatly simplifies the analysis of solar systems using immersed coils since the method of de Winter [10] can be used to assess the heat exchanger penalty. Also with the assumption of constant effectiveness, solar systems with immersed coil heat exchangers can be simulated with the use of computer simulation programs such as TRNSYS [2] and F-CHART [11]. Such a simulation is presented in Chapter 6.

The influence of the coil volumetric flow rate on heat exchanger effectiveness is important. The effectiveness is found to vary significantly over the range of flow rates tested (shown in Figure 7.0.1). This means that a solar collector and an immersed coil heat exchanger combination operating with a proportional controller may not be analyzed by the method of deWinter.

The overall heat-transfer coefficient-area product, UA, is found to be a strong function of coil fluid velocity at low velocities (<0.80 m/s). Above this fluid velocity, the function becomes weaker as the coil internal thermal resistance becomes negligible when compared to the coil external thermal resistance and the coil wall resistance (in the case of the double-wall coils). In other words,

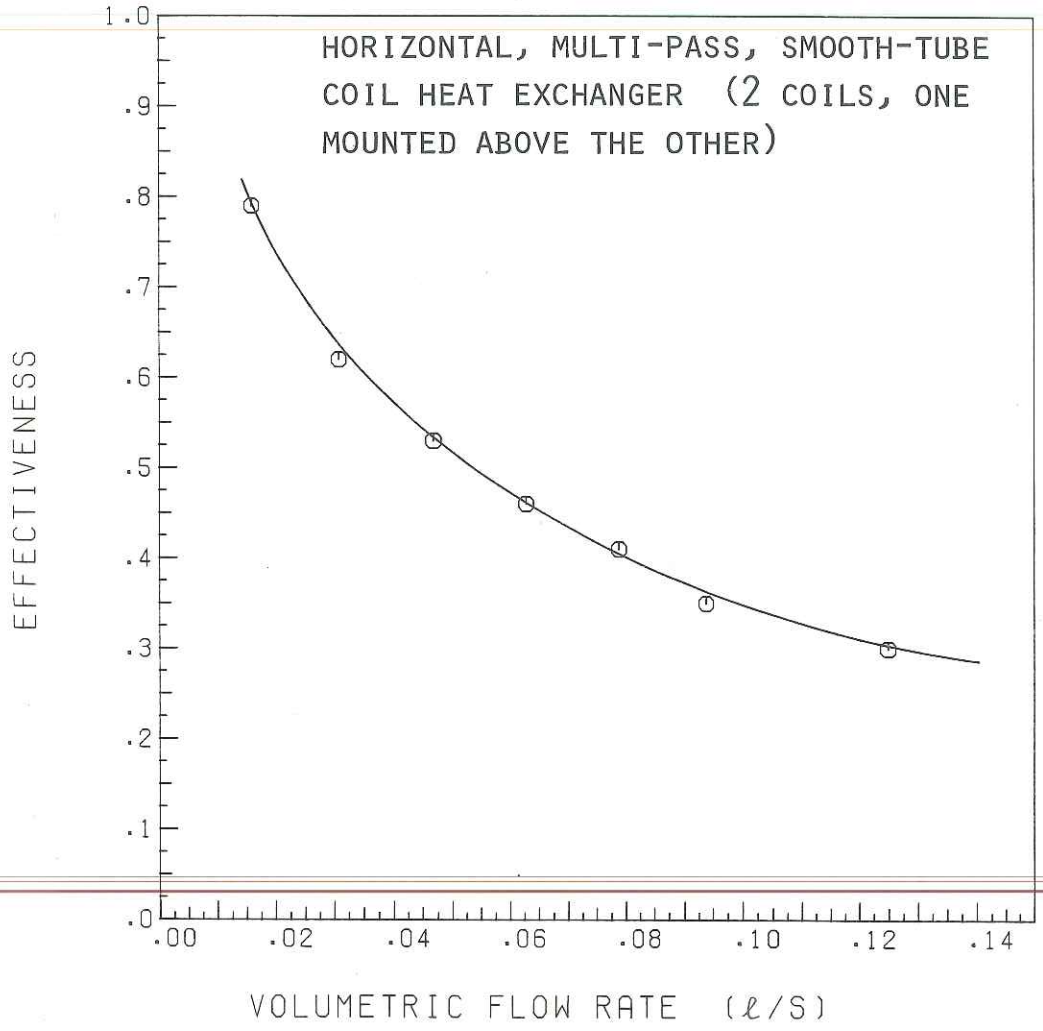

Figure 7.0.1 Coil effectiveness as a function of coil volumetric flow rate

the value of UA becomes increasingly governed by the external heat transfer coefficient and the conductance of the coil wall as the coil fluid velocity increases. A plot of this relationship is shown in Figure 7.0.2.

The overall heat-transfer coefficient-area product, UA, is also found to be a function of the temperature difference between water temperature entering the immersed coil and the tank temperature. As one might expect, UA increases with increasing temperature difference (see Figure 7.0.3). The temperature difference between the coil and the storage tank water determines the magnitude of the circulating natural convection loop. The free-convection heat transfer coefficient, h, increases with increased temperature difference and thus, so does the overall heat-transfer coefficient-area product, UA.

A series flow configuration has been found to be the most effective type of flow configuration for an immersed coil. Anytime the collector fluid is divided up to go to two or more coils within a tank, the volumetric flow rate (and fluid velocity) for each coil is reduced. By reducing the flow rate, the forced convection coefficient inside the tube is reduced and the internal film resistance of the coil is increased. The result is a reduction in the overall heat-transfer coefficient-area product, UA, and a reduction in performance.

Tests conducted on the orientation of immersed heat exchanger coils show that (with all other coil parameters being equal) the horizontal coil is superior to those sloped at 45. and 90. degrees.

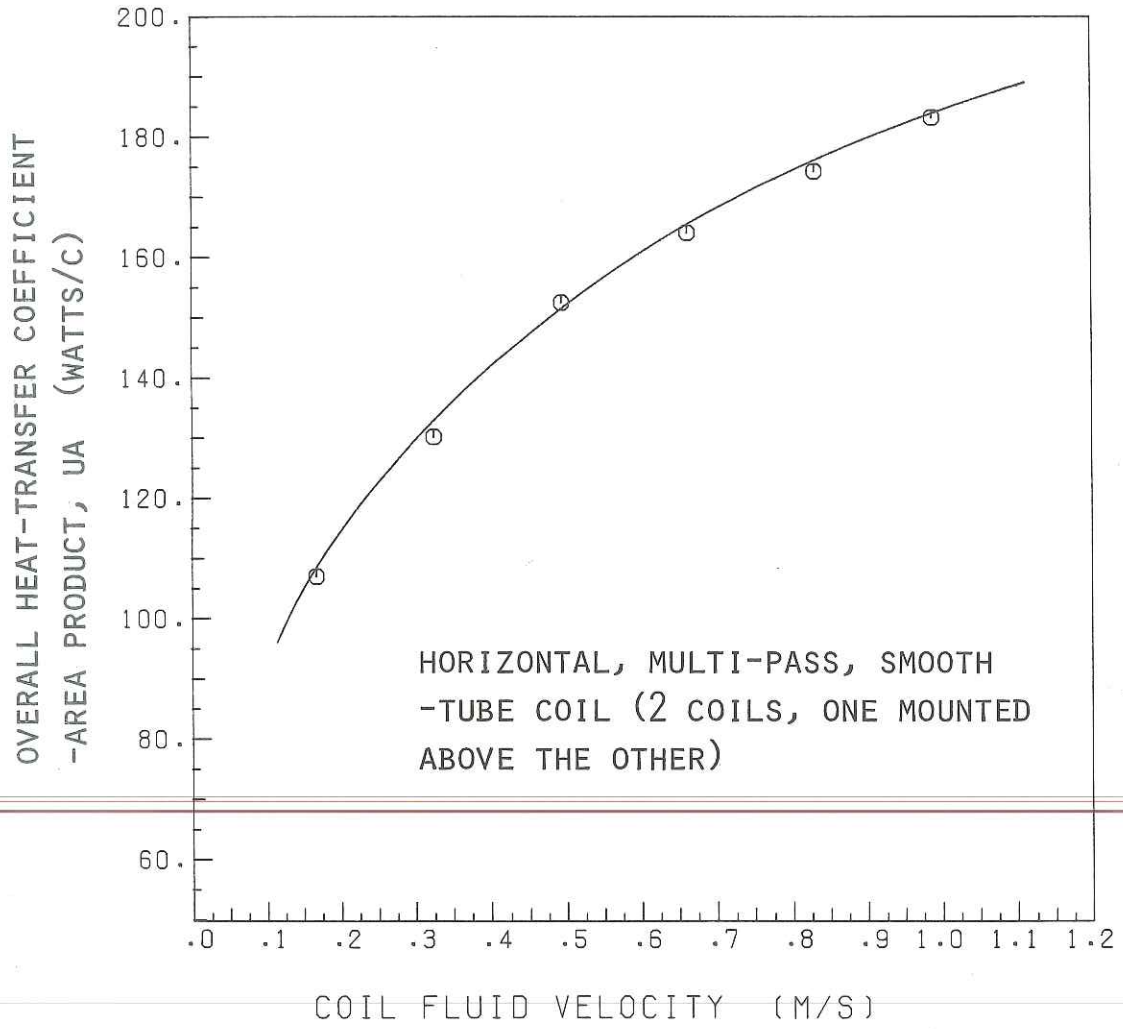

Figure 7.0.2 Overall heat-transfer coefficient-area product, UA, as a function of coil fluid velocity

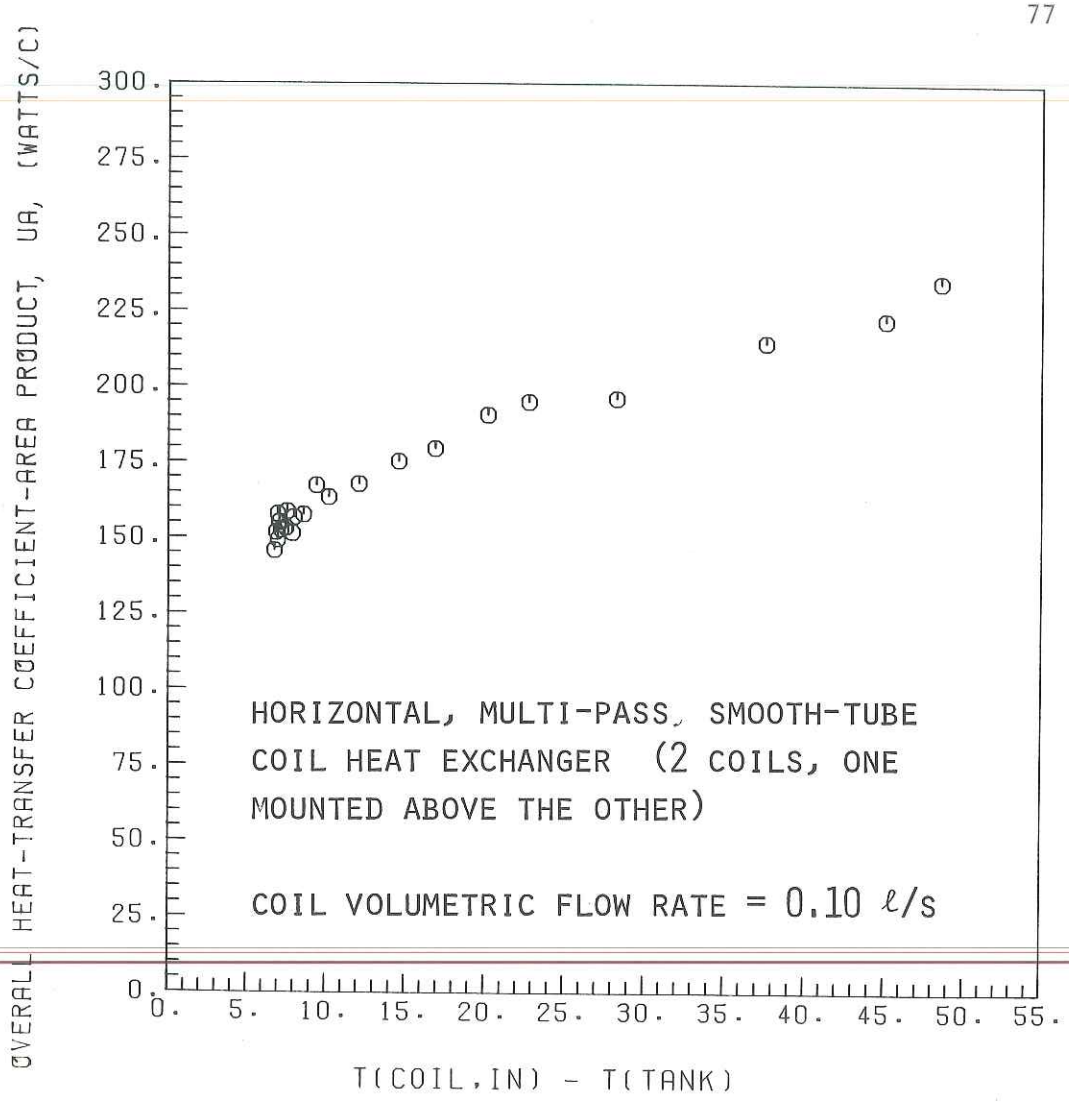

Figure 7.0.3 Overall heat-transfer coefficient-area product, UA, as a function of ($T_{c,in}$-T_{Tank})

A plot with the results of the coil orientation experiments at a coil volumetric flow rate of 0.075 ℓ/s is shown in Figure 5.6.1. The horizontal coil produces roughly 20% greater heat transfer at a given LMTD than either the coil inclined at 45. degrees or 90. degrees. Similar results were found for the other coil volumetric flow rates tested. The superiority of the horizontal configuration may result from a thinner exterior boundary layer for that orientation. This phenomenon would offer less film resistance to heat transfer.

Utilizing forced convection on the exterior of an immersed coil by moving water within the tank definitely does increase the performance of the coil. By forcibly moving the water across the coil, the exterior convection heat transfer coefficient rises and the thermal resistance on the exterior side decreases. The added benefits of simply creating a general flow within the storage tank are dubious. However, when the flow is directed with a nozzle across the immersed coils, the increase in performance is dramatic--up to a 50% increase in performance for the case tested. For the double-wall immersed coils in this study, this increase is about as good as can be expected. The increased convection heat transfer coefficient caused by the forced convection reduces the external thermal resistance enough to make the coil wall thermal resistance the major resistance. Any greater reduction in external thermal resistance will not produce major increases in the performance of the double-wall coil. For the single-wall coil (where wall resistance is negligible), greater

velocities of water within the storage tank will continue to produce dramatic increases in coil performance until the thermal resistance for the external side of the coil approaches that for the internal side. Disadvantages of this idea include parasitic power requirements, additional plumbing and increased maintenance to keep the nozzle free of deposits. For specific cases, one must determine if the overall increase in system performance outweighs the disadvantages.

Correlations of Nusselt numbers versus Raleigh numbers have been developed to aid in the design and analysis of immersed heat exchanger coils having similar configurations and dimensions of those discussed in the Physical Description and Experimental Procedure Chapter. Standard heat transfer studies indicate that the Nusselt number can be represented by an equation of the form:

$$Nu = C(Ra)^m \qquad 7.0.1$$

where C and m are constants. Because most coil applications are in the laminar region and the range of Rayleigh numbers tested was limited, the exponent m was set equal to 0.25 according to previous studies [1] of convection heat transfer from tubes. Curve-fitting produced a value for the constant, C. These correlations are based on the log-mean temperature difference between the surface of the coil and the storage tank water (from Chapter 4). The experimental data are shown in Figure 7.0.4 and the proposed correlations are:

For horizontal, multi-pass, smooth-tube coils, (two coils, one situated above the other),

$$Nu = .55\ Ra^{.25} \qquad 7.0.2$$

For horizontal, multi-pass, smooth-tube coils, (one coil),

$$Nu = .37\ Ra^{.25} \qquad 7.0.3$$

For horizontal, spiraling, finned-tube coils,

$$Nu = .34\ Ra^{.25} \qquad 7.0.4$$

For horizontal, single-pass, smooth-tube coils,

$$Nu = .74\ Ra^{.25} \qquad 7.0.5$$

The uncertainty of temperature measurements and coil volumetric flow rates produced a range for the constant C as shown in column 4 of Table 7.0.1. Column 5 of the table gives the range over which the constant, C would lie if the limit in uncertainty of all temperature and volumetric flow measurements was reached and these uncertainties affected C in the same direction. The horizontal, single-pass, smooth-tube heat exchanger produces the largest range of uncertainty due to its small size (0.057 m^2) and therefore, relatively low

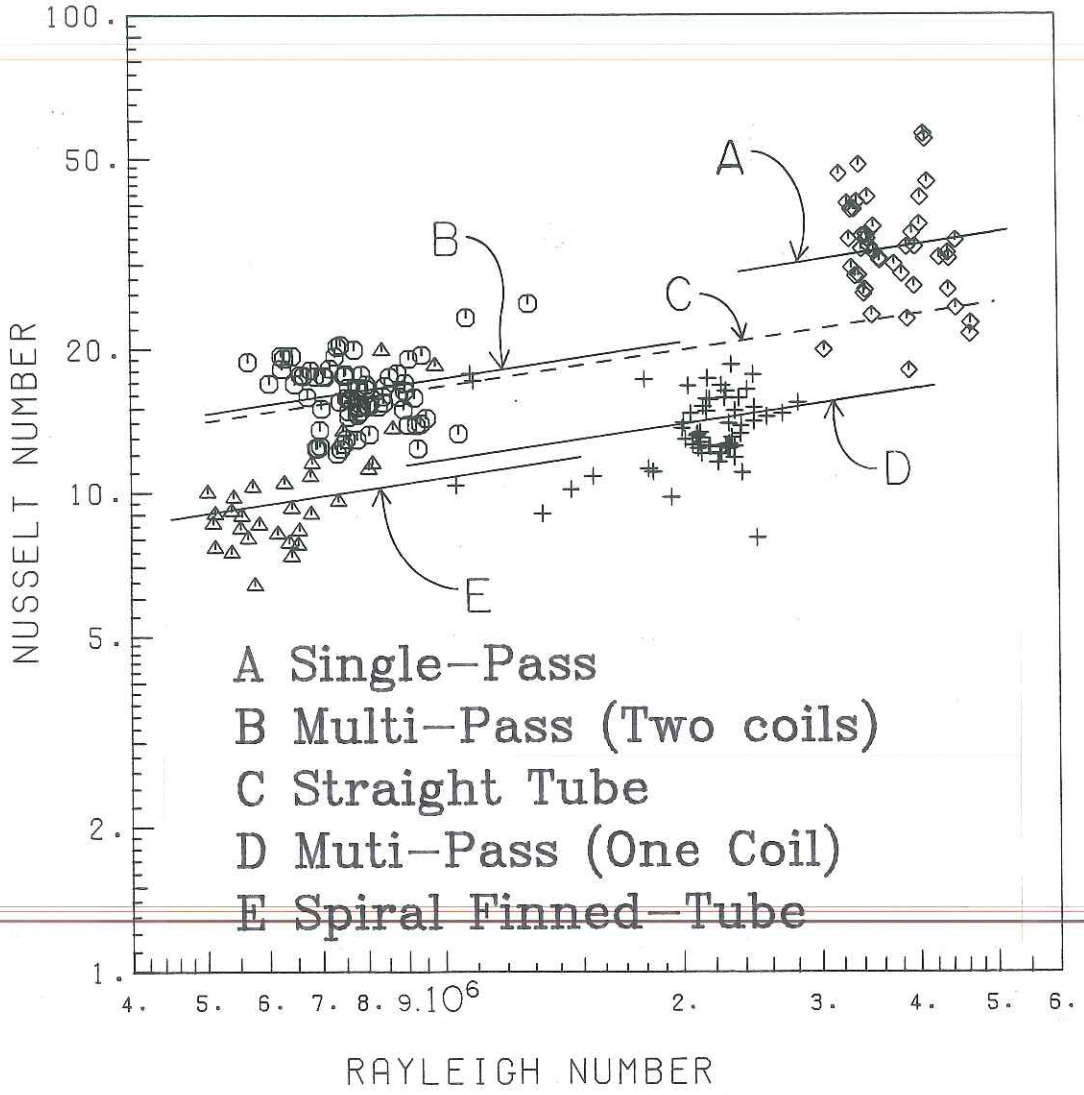

A - HORIZONTAL, SINGLE-PASS, SMOOTH-TUBE COILS (◇)

B - HORIZONTAL, MULTI-PASS, SMOOTH-TUBE COILS (TWO COILS, ONE MOUNTED ABOVE THE OTHER) (⊙)

C - HORIZONTAL, STRAIGHT TUBE [1]

D - HORIZONTAL, MULTI-PASS, SMOOTH-TUBE COILS (ONE COIL) (+)

E - HORIZONTAL, SPIRALING, FINNED-TUBE COILS (△)

Figure 7.0.4 Nusselt number as a function of Rayleigh number for four coil configurations (with a comparison to literature [1])

Table 7.0.1 Variation in Observations and Variations Due to Uncertainties in Measurements

Coil Configuration	Constant, C	Number of Observations	Variation Among Observations	Worst Case Condition
1)	.55	72	$.42 < C < .75$	$.31 < C < .98$
2)	.37	60	$.24 < C < .54$	$.23 < C < .65$
3)	.34	30	$.22 < C < .44$	$.18 < C < .68$
4)	.74	46	$.49 < C < 1.02$	$.49 < C < 1.09$

1) Horizontal, multi-pass, smooth-tube coils, (two coils, one situated above the other)

2) Horizontal, multi-pass, smooth-tube coils, (one coil)

3) Horizontal, spiraling, finned-tube coils

4) Horizontal, single-pass, smooth-tube coils

temperature difference between the inlet and outlet (~3°C). The uncertainty in temperature measurement may be as much as 25% of the measured temperature difference in this case.

For the horizontal, multi-pass, smooth-tube coil (2 coils, one mounted above the other) configuration, two sets of separate tests conducted eight months apart yielded essentially the same result for the constant C. One set of tests produced a value of .56 while the other set of tests produced a value of .55.

When using these correlations to predict coil performance, the less similar the coil to the described coils, the less reliable the correlation. They will however, provide guidelines for coil design and analysis for many applications. More studies are needed to expand the number of correlations to describe the performance of other configurations. An example of the use of the preceeding equations is given in Appendix B. This sample problem predicts the effectiveness of an immersed coil heat exchanger and the heat exchanger penalty for a typical collector system.

The constant, C (from equation 7.0.1) is a relative evaluation of the convection heat transfer coefficient for a given temperature difference between the coil surface temperature and the tank temperature. Comparing C for each of the immersed coil configurations reveals some interesting facts.

The horizontal, single-pass, smooth-tube coil (hereafter described as single-pass coil) produces the highest exterior convection heat transfer coefficient of the coils tested (for a given tempera-

ture difference). This coil approximates a horizontal, straight tube. The horizontal multi-pass, smooth-tube coil (2 coils, one mounted above the other; hereafter described as multi-pass, 2 coil) will produce a convection heat transfer coefficient which is about 75% of that of the single-pass coil at the same temperature difference. The horizontal, multi-pass, smooth-tube coil (1 coil; hereafter described as multi-pass, 1 coil) and the horizontal, spiraling, finned coil (finned coil) produce roughly the same convection heat transfer coefficient at about 50% of that for the single-pass coil and about 65% of that for the multi-pass, 2 coil configuration (for a given temperature difference). The poor convection coefficient of the finned coil may be due to its tight construction (see Figure 2.1.2b) and/or narrow fin spacing (4 fins/cm of tube length). The relatively large surface area of the finned coil (0.73 m^2) makes up for the relatively low convection heat transfer coefficient making its external thermal resistance and hence performance approximately equal to that of the multi-pass, 2 coil configuration (surface area = 0.45 m^2). Measurements show that for a given temperature difference, the heat transfer rate for both configurations is about the same (within about 10%). This means that the finned coil mounted in one of the two portals of the storage tank is doing nearly the same job as the multi-pass, 2 coil configuration which is mounted in 2 portals. Placing a finned coil in each of the two mounting portals would significantly increase system performance.

When comparing the constant, C for the multi-pass, 1 coil and multi-pass, 2 coil we notice that the convection heat transfer coefficient increases by about 50% when the multi-pass configuration's surface area doubles. Hence the exterior thermal resistance is reduced by a third and the multi-pass, 2 coil configuration performs roughly 3 times better than the multi-pass, 1 coil configuration at the same temperature difference.

The multi-pass, 1 coil and 2 coil configurations approximate tube banks. One would expect that the fewer the tubes (from 2 coils to 1 coil), the closer the convection heat transfer coefficient would approach that of the single-pass coil (for a given temperature difference). In fact the opposite is true. The cause for this anomaly is unknown.

Two effects that govern coil performance appear to be occurring due to the convection currents surrounding the coil. The first effect is that of hydrodynamic interaction. The convection currents caused by the lower portion of the coil will rise to add to the convection currents produced by the upper portion of the coil. The effect is to increase the average exterior free-convection coefficient and in doing so, increase coil performance. The second effect is that of thermal interaction. The convection currents described above are warmer than the surrounding storage tank water. This reduces the temperature difference between the immersed coil and the surrounding water and produces a decrease in coil performance. Which of these effects is greater is probably a function of coil

design and temperature differences.

Summary

A number of conclusions can be made from this study regarding improved immersed coil and water heater design. They are:

1) Immersed coils constructed to produce the least interaction with other parts of the coil appear to produce the greatest convection heat-transfer coefficients. This would suggest that a coil be constructed so that it lies in nearly the same horizontal plane when mounted in the storage tank. To accommodate an immersed coil of adequate size constructed in this manner may require a storage tank with increased horizontal dimensions along with a decreased height to maintain the same capacity.
2) The coil wall thermal resistance should be kept to a minimum. Wherever building codes permit, single-wall copper coils should be used. If double-wall immersed coils must be used, they should be constructed with maximum contact between the inner and outer tubes. Minimum tolerances between the tube sizes and press-fitting the tubes together will help. The use of a "thermal" grease (such as Dow 340) at the coil wall interface can significantly reduce the thermal contact resistance.
3) Any movement of water through the storage tank should be directed across the immersed coil. If no auxillary pump is used to create a movement of water within the tank, the replacement water required for a load draw should enter

the tank across the coil.

4) Coil fluid velocities should be high enough to minimize the internal thermal resistance. There is a trade-off here; as the coil fluid velocity increases, the pressure drop across the coil and pumping costs increase.

5) The use of fins on the exterior side of the coil to increase surface area and thus reduce external thermal resistance is desirable. Caution should be exercised in fin spacing. Closely spaced fins (4 fins/cm for the finned coil in this study) appear to reduce the convection heat transfer coefficient.

6) Keeping items 2, 4, and 5 in mind, the external, coil wall and internal thermal resistances should be approximately equal.

7) The immersed coil should be positioned at or near the bottom of the storage tank to fully utilize the thermal capacity of the storage tank.

APPENDIX A

EXPERIMENTAL EQUIPMENT

Hot Water Source Tank:

Manufacturer: R. Edmunds and Sons.

Capacity: 300. ℓ

Heating element: 3000 W, dry electric element

Serial number: 62890

Thermal Storage Tank:

Manufacturer: A. O. Smith Corp.

Model: Conservationist Solar Water Heater, #JTHE100

Serial number: 888-M-79-11293

Capacity: 340. ℓ (measured)

Average overall heat-transfer coefficient: 0.89 $\frac{W}{m^2 °C}$
(while experimentally equipped)

Insulation: Fiberglass wool, 0.06 m thick sheath

Tank: height = 1.40 m

diameter = 0.62 m

mass = 102. kg

Case: height = 1.48 m

diameter = 0.74 m

heat transfer area to environment = 3.70 m^2

(The bottom is well insulated and is not considered in the heat transfer area.)

Rotameter: (2)

Manufacturer: Brooks Instrument Company, Inc.

Type: 9-1110-MS

Serial number: 6208-38773/72

Range: 0.0 ℓ/s - 0.32 ℓ/s

Pump: (2)

Manufacturer: Little Giant Pump Company

Rating: 115 v, 3.2 A, 370 W, 1 phase

Type: Centrifugal impeller

Maximum capacity: 0.55 ℓ/s (no head)

Chart Recorder:

Manufacturer: Minneapolis-Honeywell Regulator Company

Type: 12 channel, adjusted for Cu-Cn thermocouples

Serial number: 5397-N

Model number: 153X64P12-X-141

Range: -20.°C to 120.°C

Digital Thermometer:

Manufacturer: Fluke

Type: 10 channel, adjusted for Cu-Cn thermocouple

Serial number: 2320014

Model number: 2176A

APPENDIX B Sample Problem

Design programs for solar heating systems such as FCHART [12] or TRNSYS [2] require a value of heat exchanger effectiveness for the collector-storage heat exchanger. Storage tanks utilizing immersed coil heat exchangers are often used in solar heating systems and can be incorporated into these design programs provided one can predict coil effectiveness. The following is an example of such a prediction based on a heat transfer correlation presented in Chapter 7.

Sample Problem

Water flows through an immersed coil of a water storage tank in a solar heating system. Determine the coil effectiveness and calculate the heat exchanger penalty factor, F'_R/F_R [11] for the system with the following specifications.

Coil Data:

Type: horizontal, multi-pass, smooth-tube (double-wall construction)

Wall thermal resistance: 0.0023 °C/W (based on a contact coefficient of 1200. $W/m^2°C$)

Area: outside 0.45 m^2, inside 0.31 m^2

Diameters (tube): ID 0.011 m, OD 0.016 m

Collector Data:

Area: $6.0\ m^2$

$F_R U_L$: $3.75\ W/m^2{}^\circ C$

Collector-coil loop volumetric flow rate: $0.10\ \ell/s = 0.10\ kg/s$

Temperature Data:

Storage tank temperature: $44.0^\circ C$

Temperature of water entering the coil: $55.0^\circ C$

Solution

It is necessary to first guess an average coil outside surface temperature and a coil exit temperature and later check these assumptions. The coil surface temperature is assumed to be $49.0^\circ C$ and the coil exit temperature is assumed to be $51.5^\circ C$.

Properties: Source [1]

Water, $T_f = 46.5^\circ C$

$\beta = 3.79 \times 10^{4}\ {}^\circ K^{-1}$

$\mu = 5.85 \times 10^{-4}\ kg\ m^{-1} s^{-1}$

$k = 0.641\ W\ m^{-1}\ {}^\circ C^{-1}$

$\nu = 6.11 \times 10^{-7}\ m^2 s^{-1}$

$\alpha = 1.54 \times 10^{-7}\ m^2 s^{-1}$

Water, $T_{c,ave} = 53.3^\circ C$

$\mu = 5.24 \times 10^{-4}\ kg\ m^{-1} s^{-1}$

$k = 0.648\ W\ m^{-1}\ {}^\circ C^{-1}$

$Pr = 3.37$

$$C_p = 4180.\ J\ kg^{-1}\ °C^{-1}$$

Analysis:

$$Ra_x = \frac{g\beta\ (T_S - T_T)_x^3}{\nu\alpha}$$

$$= \frac{(9.8 ms^{-2})(3.79x10^{-4} °K^{-1})(5°K)(0.016m)^3}{(6.11x10^{-7} m^2 s^{-1})(1.54x10^{-7} m^2 s^{-1})}$$

$$= 8.08 \times 10^5$$

Using Eq. 7.0.2,

$$Nu = .55(8.08 \times 10^5)^{.25} = 16.5$$

and,

$$h_o = \frac{Nu\ k}{D_o} = \frac{(16.5)(0.641\ W\ m^{-1}\ °C^{-1})}{(0.016\ m)} = 661.\ W\ m^{-2}\ °C^{-1}$$

To calculate effectiveness, we must determine the internal convection coefficient based on the Dittus-Boelter correlation for flow through a tube [1].

$$Re = \frac{4\ \dot{m}}{\pi D_i \mu} = \frac{4\ (0.10\ kg\ s^{-1})}{\pi(0.011\ m)(5.24x10^{-4}\ kg\ m^{-1}\ °C^{-1})} = 22100.$$

$$Nu_i = 0.23\ Re^{.8}\ Pr^{.4} = .023(22100)^{.8}(3.37)^{.4} = 111.8$$

$$h_i = \frac{(111.8)(0.648\ W\ m^{-1}\ °C^{-1})}{(0.011\ m)} = 6600.\ W\ m^{-2}\ °C^{-1}$$

Now to calculate the overall heat-transfer coefficient-area product, UA, we use,

$$UA = \frac{1}{\frac{1}{h_o A_o} + R_w + \frac{1}{h_i A_i}}$$

$$= \frac{1}{\frac{1}{(661.\ Wm^{-2}°C^{-1})(0.45m^2)} + 0.0023°C\,W^{-1} + \frac{1}{(6600\ Wm^{-2}°C^{-1})(0.31m^2)}}$$

$$= 163.\ W\ °C^{-1}$$

Due to the assumption of a constant average temperature along the cold side (exterior side) of the heat exchanger coil, it may be considered to have infinite capacity. The expression for effectiveness [1] then becomes,

$$\varepsilon = 1-\exp\left[\frac{-UA}{\dot{m}\,C_p}\right] = 1-\exp\left[\frac{(-163.\ W°C^{-1})}{(0.10\ kg\ s^{-1})(4180.\ J\ kg^{-1}°C^{-1})}\right]$$

$$= 0.32$$

Now to check the assumptions of $T_s = 49.0°C$ and $T_{c,out} = 51.5°C$:

$$\varepsilon = \frac{q_{act}}{q_{max}} = \frac{h_o A_o (T_s - T_T)}{\dot{m}\,C_p\,(T_{c,in} - T_T)} = \frac{T_{c,in} - T_{c,out}}{T_{c,in} - T_T}$$

therefore,

$$T_s = \frac{\dot{m}\, C_p\, (T_{c,in} - T_T)\varepsilon}{h_o A_o} + T_T$$

$$= \frac{(0.10\ kg\ s^{-1})(4180.\ J\ kg^{-1}{}^{\circ}C^{-1})(55.0^{\circ}C-44.0^{\circ}C)(0.32)}{(661.\ W\ m^{-2}\ {}^{\circ}C^{-1})(0.45\ m^2)} + 44.0^{\circ}C$$

$$= 49.0^{\circ}C \quad \{49.0^{\circ}C\}$$

and,

$$T_{c,out} = T_{c,in} - \varepsilon(T_{c,in} - T_T$$

$$= 55.0^{\circ}C-0.32(55.0^{\circ}C-44.0^{\circ}C)$$

$$= 51.5^{\circ}C \quad \{51.5^{\circ}C\}$$

Now to calculate the heat exchanger penalty factor,

$$\frac{F'_R}{F_R} = \frac{1}{1 + \left[\frac{A_C\ F_R\ U_L}{(\dot{m}\ C_p)_c}\right]\left[\frac{1}{\varepsilon} - 1\right]}$$

$$= \frac{1}{1 + \left[\frac{(6.0m^2)(3.75\ Wm^{-2}{}^{\circ}C^{-1})}{(0.10\ kgs^{-1})(4180.\ J\ kg^{-1}{}^{\circ}C^{-1})}\right]\left[\frac{1}{.32} - 1\right]}$$

$$= 0.90$$

This represents the penalty in collector performance incurred because the coil heat exchanger causes it to operate at higher temperatures than it otherwise would. With this coil, 11% (i.e., 1/0.90 - 1) greater collector area would be required to deliver the same energy compared to a system without the heat exchanger.

APPENDIX C Measurement of the Contact Coefficient of Double-Wall Immersed Coils

The construction of the double-wall coils is simply a copper tube press-fitted around a slightly smaller diameter copper tube. The thermal conductivity of the copper is very high (386 $\frac{W}{m°C}$ so the thermal resistance due to the copper can be ignored. The thermal contact resistance ($\frac{1}{h_c A_c}$) between the two tubes can be significant. The thermal contact coefficient, h_c, is measured as follows:

The temperature of the exterior surface of coil being tested was measured near the entrance and exit of the coil by attaching thermocouples to it. Small grooves were etched into the surface and the thermocouples were placed in these grooves. The joint was then soldered, completely covering the thermocouple. Wires leading to these joints were insulated to minimized fin effects. The temperature of the coil water was measured at the entrance and exit along with the coil volumetric flow rate and tank temperature as described in Chapter 2. In these experiments, all temperature measurements were made when large temperature differences were present to minimize errors.

The expression for the contact coefficient [1] is,

$$h_c = \frac{1}{R_w A_c} \qquad \text{A.1}$$

where A_c is the area at the interface between the inner and outer

tubes of the coil wall. The tube diameter at the interface is 0.0127 m for all coils in this study. The thermal circuit for analysis is,

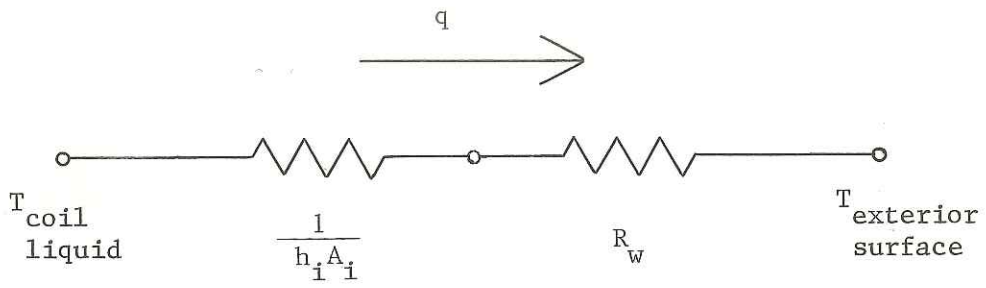

and the equation for wall thermal resistance is,

$$R_w = \frac{LMTD^*}{q} - \frac{1}{h_i A_i} \qquad A.2$$

With $R_w = 0.$ for the single-wall coil, equation A.2 can be manipulated into the form:

$$h_i = \frac{q}{(LMTD)(A_i)} \qquad A.3$$

---

*Since the temperature of the coil surface and the temperature of the coil water vary along the length of the coil, it is appropriate to use a log-mean temperature difference between the coil exterior surface temperature and the coil water temperature.

The internal convection coefficient, h, was determined over a range of coil volumetric flow rates for the single-wall coil and then scaled according to the Dittus-Boelter correlation for flow through tubes [1] to account for the different internal diameters and coil flow rates between the single-wall and double-wall coils. Assuming constant fluid properties, this relationship is:

$$h_i = \left(\frac{D'}{D}\right)^{1.8} \left(\frac{\dot{m}}{\dot{m}'}\right)^{.8} h_i' = 1.69 \left(\frac{\dot{m}}{\dot{m}'}\right)^{.8} h_i' \qquad \text{A.4}$$

where the prime represents those measurements taken with the single-wall coil.

Tests were conducted on the horizontal, multi-pass, smooth-tube and horizontal spiraling, finned-tube coils (both described in Chapter 2). The wall thermal resistance for both of these coils is not negligible due to significant contact resistance at the interface between the inner and outer tubes. Using equations A.1 and A.2 with the internal convection coefficient (scaled from the single-wall coil tests), the contact coefficients and thermal wall resistances were determined for the double-wall coils.

The contact coefficient for the wall of the horizontal, multi-pass, smooth-tube coil was found to be 1300. $\pm$ 140. W/m^2 °C (wall thermal resistance = 0.0047 $\pm$ 0.0005 °C/W). The uncertainty in this is due to the uncertainty in temperature measurements and the fact that about 15% of the length of the outer tube is not press-fitted to the inner tube. The degree of contact between the inner

and outer walls is uncertain in this area.

The contact coefficient for the coil configuration consisting of two horizontal, multi-pass, smooth-tube coils is the same as that for one coil due to identical construction. The wall thermal resistance is 0.0023 $\pm$ 0.0002 °C/W.

The contact coefficient of the wall of the horizontal, spiraling, finned-tube coil was found to be 4000. $\pm$ 400. W/m^2 °C (wall thermal resistance = 0.0018 $\pm$ 0.0002 °C/W). The uncertainty in this measurement is due to the uncertainty in temperature measurement only (since this coil is evenly press-fitted throughout its length).

A worst case coil double-wall resistance would be that of no metal to metal contact between the inside and outside tubes of the coil wall. The dimensions of the tubes used in the coils of this study would allow a 0.0006 m air gap between the two tubes if they were not press-fitted together. The resulting wall thermal resistance for the horizontal, multi-pass, smooth-tube coil would be 0.113 °C/W. This is well above its measured value of wall resistance.

APPENDIX D. Computer program listings

```
C      THIS PROGRAM EVALUATES IMMERSED COIL HEAT EXCHANGER
C  PERFORMANCE FOR SMOOTH-TUBE COIL OF THE TYPE COMMONLY
C  FOUND IN SOLAR WATER HEATERS.
C      INPUTS REQUIRED FOR THIS COMPUTER PROGRAM ARE:
C
C         DIN = INSIDE TUBE DIAMETER  (METERS)
C         DOUT = OUTSIDE TUBE DIAMETER  (METERS)
C         L = LENGTH OF TUBE  (METERS)
C         R = COIL WALL THERMAL RESISTANCE  (C/W)
C         POINTS = THE NUMBER OF DATA SETS
C
C         TTANK = STORAGE TANK TEMPERATURE  (C)
C         TINLET = TEMPERATURE OF THE WATER ENTERING THE COIL  (C)
C         TOUT = TEMPERATURE OF THE WATER LEAVING THE COIL  (C)
C         MFLOW = COIL VOLUMETRIC (MASS) FLOW RATE  (KG/S)
C         HBARIN = AVERAGE COIL INTERNAL CONVECTION HEAT TRANSFER
C                  COEFFICIENT (DETERMINED EXPERIMENTALLY BY METHODS
C                  EXPLAINED IN APPENDIX C)  (W/M**2 C)
C
C
C             *** INTERNAL TERMINOLOGY ***
C
C
C         AOUT = COIL EXTERNAL SURFACE AREA
C         AIN = COIL INTERNAL SURFACE AREA
C         TFLOW = AVERAGE TEMPERATURE OF THE COIL FLUID
C         CP = SPECIFIC HEAT OF WATER
C         MUFLOW = DYNAMIC VISCOSITY OF WATER
C         QEXP = HEAT TRANSFER RATE FROM THE COIL TO THE TANK
C         LMTD = LOG-MEAN TEMPERATURE DIFFERENCE
C                BETWEEN THE COIL FLUID AND THE STORAGE TANK
C         UAEXP = OVERALL HEAT-TRANSFER COEFFICIENT-AREA PRODUCT
C                OF THE IMMERSED COIL
C         EFFECT = COIL EFFECTIVENESS
C         REYFLW = REYNOLDS NUMBER OF THE COIL FLUID
C         HBAREX = EXTERNAL CONVECTION HEAT TRANSFER COEFFICIENT
C         TSURF = IMMERSED COIL SURFACE TEMPERATURE
C         TFILM = FILM TEMPERATURE AT THE COIL EXTERNAL SURFACE
C         RHOFLM = DENSITY OF WATER
C         MUFILM = DYNAMIC VISCOSITY AT THE FILM TEMPERATURE
C         KFILM = CONDUCTIVITY OF WATER AT THE FILM TEMPERATURE
C         PRFILM = PRANDTL NUMBER AT THE FILM TEMPERATURE
C         NUEX = COIL EXTERNAL NUSSELT NUMBER
C         BETA = VOLUME COEFFICIENT OF EXPANSION
```

```
C          FLMTD = LOG-MEAN TEMPERATURE DIFFERENCE BETWEEN THE
C                  COIL SURFACE AND THE STORAGE TANK WATER
C          GR = GRASHOF NUMBER
C          RAY = RAYLEIGH NUMBER
C
C
      REAL NUEX,MFLOW,LMTD,L
      REAL KFILM,MUFLOW,MUFILM
      INTEGER POINTS
      WRITE(*,100)
      WRITE(*,100)
      WRITE(*,110)
      READ(*,*) R
      WRITE(*,100)
      WRITE(*,90)
      WRITE(*,100)
      READ(*,*)DIN,POINTS,L,DOUT
      WRITE(*,50)
      WRITE(*,100)
      AFLOW=0.
      AOUT=3.1416*DOUT*L
      AIN=3.1416*DIN*L
      WRITE(*,10)
      WRITE(*,20) AOUT,AIN
      WRITE(*,100)
      WRITE(*,100)
      WRITE(*,120)
      WRITE(*,130)
C
C  CALCULATION LOOP
C
      DO 2 N=1,POINTS
      READ(*,*)TTANK,TINLET,TOUT,MFLOW,HBARIN
C
C     EVALUATE INTERNAL PROPERTIES
C
      TFLOW=(TINLET+TOUT)/2.0
      CP=4179.
      MUFLOW=.067*(TFLOW*1.8+32.)**(-1.005)
C
C  EVALUATE EXPERIMENTAL DATA
C
      QEXP=CP*MFLOW*(TINLET-TOUT)
      LMTD=(TINLET-TOUT)/ALOG((TINLET-TTANK)/(TOUT-TTANK))
      UAEXP=QEXP/LMTD
      EFFECT=(TINLET-TOUT)/(TINLET-TTANK)
      REYFLW=(4.*MFLOW)/(3.1416*DIN*MUFLOW)
C
C  FREE CONVECTION FROM EXTERIOR OF COIL
C
```

```
      HBAREX=1./((1./UAEXP-(R)-1./(HBARIN*AIN))*AOUT)
C
C     EVALUATE EXTERNAL PROPERTIES
C
      TSURF=TTANK+QEXP/(HBAREX*AOUT)
      TFILM=(TSURF+TTANK)/2.0
      RHOFLM=1008.-.4238*TFILM
      MUFILM=.067*(TFILM*1.8+32.)**(-1.005)
      KFILM=.3739*(TFILM*1.8+32.)**.1133
      PRFILM=(CP*MUFILM)/KFILM
      NUEX=HBAREX*DOUT/KFILM
      BETA=(7.143E-06)*TFILM+(9.0143E-05)
      FLMTD=(UAEXP/(HBAREX*AOUT))*LMTD
      GR=9.81*BETA*(FLMTD)*(DOUT**3)*(RHOFLM**2)/
     C MUFILM**2
      RAY=GR*PRFILM
      IF (MFLOW.EQ.AFLOW) GO TO 3
      WRITE(*,50)
3     AFLOW=MFLOW
C
C  OUTPUT
C
      WRITE(9,80)MFLOW,EFFECT,LMTD,QEXP,UAEXP,REYFLW,NUEX,
     C RAY,HBAREX,HBARIN
      WRITE(6,80)MFLOW,EFFECT,LMTD,QEXP,UAEXP,REYFLW,NUEX,
     C RAY,HBAREX,HBARIN
2     CONTINUE
C
C  FORMATTING
C
10    FORMAT(5X,'IMMERSED COIL EXTERNAL SURFACE AREA ',
     CT86,'IMMERSED COIL INTERNAL SURFACE AREA ')
20    FORMAT(T15,'= ',F3.2,' SQUARE METERS',T95,'= ',F3.2,
     C' SQUARE METERS')
110   FORMAT(5X,'WHAT IS THE COIL WALL THERMAL ',
     C'RESISTANCE (C/W)?')
120   FORMAT(T2,'MASSFLOW',T14,'EFFECT.',T25,'LMTD',T33,'HEAT FLOW',
     CT46,'UA EXPER.',T58,' REYN. # ',T71,'NUSSELT-OUT',T86,
     C'RAYLEIGH NO.',T102,'H AVE.-OUT',T116,'H AVE.-IN')
130   FORMAT(T2,'KG/S',T25,'C',T33,'WATTS',T46,'WATTS/C',
     CT102,'------WATTS/M**2 C--------')
90    FORMAT(5X,'ADD THE MEASURED DATA NOW')
100   FORMAT(' ')
80    FORMAT(T4,F4.3,T15,F3.2,T25,F4.1,T34,F6.0,T48,F5.1,T60,F7.1,T74,
     CF7.2,T89,E10.5,T104,F7.1,T117,F8.1)
50    FORMAT(126('*'))
      STOP
      END
```

IMMERSED COIL EXTERNAL SURFACE AREA
= .45 SQUARE METERS

IMMERSED COIL INTERNAL SURFACE AREA
= .31 SQUARE METERS

MASSFLOW KG/S	EFFECT.	LMTD C	HEAT FLOW WATTS	UA EXPER. WATTS/C	REYN. #	NUSSELT-OUT	RAYLEIGH NO.	H AVE.-OUT -----WATTS/M**2 C------	H AVE.-IN
.075	.43	10.6	1849.	174.8	15339.6	20.40	.74264+006	803.9	4798.0
.075	.41	9.1	1504.	165.5	15471.6	18.19	.71946+006	719.6	4798.0
.075	.41	8.2	1348.	165.1	15651.6	18.06	.67978+006	716.3	4798.0
.075	.41	7.5	1222.	163.4	15867.7	17.64	.65943+006	701.7	4798.0
.075	.42	7.2	1222.	170.4	16107.7	19.13	.62915+006	762.5	4798.0
.075	.40	6.7	1066.	160.1	16335.8	16.88	.64855+006	674.8	4798.0
.075	.39	6.5	1003.	155.1	16600.0	15.86	.67420+006	635.3	4798.0
.075	.41	6.2	1034.	166.7	16852.1	18.19	.62551+006	729.9	4798.0
.075	.41	6.3	1034.	164.0	17116.3	17.58	.66592+006	706.8	4798.0
.075	.42	6.0	1034.	172.4	17380.4	19.38	.62440+006	781.0	4798.0
.100	.37	22.6	4430.	196.1	22389.4	24.94	.12868+007	975.2	6040.0
.100	.37	16.2	3092.	190.7	21717.1	23.28	.10703+007	916.2	6040.0
.100	.34	11.9	2089.	175.2	21365.0	19.43	.94135+006	768.8	6040.0
.100	.33	10.0	1672.	167.7	21493.0	17.78	.87583+006	706.2	6040.0
.100	.32	8.4	1379.	163.3	21637.1	16.86	.80038+006	671.9	6040.0
.100	.33	7.7	1295.	167.2	21925.2	17.58	.75054+006	702.3	6040.0
.100	.31	7.2	1128.	157.5	22213.3	15.69	.76327+006	628.3	6040.0
.100	.31	6.7	1045.	156.6	22501.5	15.50	.74125+006	622.0	6040.0
.100	.30	6.6	1003.	151.3	22837.7	14.56	.78132+006	585.4	6040.0
.100	.31	6.3	961.	153.1	23173.9	14.82	.76126+006	597.2	6040.0
.125	.28	16.5	2873.	174.2	23726.1	19.08	.90519+006	737.6	7221.0
.125	.29	12.8	2298.	179.9	23426.2	20.24	.73522+006	786.0	7221.0
.125	.27	10.6	1776.	167.4	23506.2	17.55	.70613+006	684.7	7221.0
.125	.25	9.2	1410.	153.6	23766.1	14.98	.70224+006	586.9	7221.0
.125	.24	8.3	1201.	144.8	24086.0	13.52	.69878+006	531.3	7221.0
.125	.28	7.5	1306.	174.6	24446.0	18.81	.56705+006	741.1	7221.0
.125	.23	7.2	993.	137.7	24885.9	12.38	.69172+006	489.3	7221.0
.125	.27	6.9	1149.	165.5	25305.9	16.94	.60316+006	670.8	7221.0
.125	.23	6.8	940.	139.1	25786.0	12.52	.70117+006	497.4	7221.0
.125	.23	6.4	888.	138.5	26206.1	12.40	.69504+006	493.9	7221.0

Sample output

```
*          ---------- TRNSYS SIMULATION ----------
*
*             *** WITHOUT STORAGE TANK LOAD ***
*
*       THIS TRNSYS DECK IS A SIMULATION OF A THERMAL STORAGE
*   TANK WITH AN IMMERSED COIL. AN EXTERNAL, SENSIBLE HEAT
*   EXCHANGER WITH CONSTANT EFFECTIVENESS IS SUBSTITUTED FOR
*   THE IMMERSED COIL SINCE TRNSYS HAS NO PROVISIONS TO
*   DIRECTLY MODEL AN IMMERSED COIL HEAT EXCHANGER. THE
*   SIMULATION OUTPUT IS COMPARED TO EXPERIMENTAL DATA.
*
*
*                    *** TERMINOLOGY ***
*
*          E = EFFECTIVENESS
*          MFL = IMMERSED COIL MASS (VOLUMETRIC) FLOW RATE
*          TI = INITIAL TANK TEMPERATURE
*          TA = ENVIRONMENT TEMPERATURE
*          TIH = INITIAL TEMPERATURE OF THE FLUID LEAVING
*                THE COIL
*
*                *** TIME STEP INPUTS ***
*
*          --- TEMPERATURE OF THE WATER ENTERING THE COIL
*          --- STORAGE TANK TEMPERATURE (FOR COMPARISON
*              PURPOSES ONLY)
*          --- TEMPERATURE OF THE WATER LEAVING THE COIL
*              (FOR COMPARISON PURPOSES ONLY)
*
*  SET STARTING TIME, STOPPING TIME AND INTERVAL
*
SIMULATION 0.0 11.5 .1
CONSTANTS E=.320 MFL=360. TI=29.5 TA=19.8 TIH=57.8
*
*  INPUT TEMPERATURE DATA
*
UNIT 9  TYPE 9  DATA READING (FORMATTED)
PARAMETERS 4
3 .50 0 1
(T3,F4.1,2X,F4.1,2X,F4.1)
*
*  SENSIBLE HEAT EXCHANGER
*
UNIT 5  TYPE 5  HEAT EXCHANGER
PARAMETERS 4
4 E 4179. 4179.
INPUTS 4
9,2 0,0 4,1 0,0
TI MFL TIH MFL
*
```

```
*  THERMAL STORAGE TANK
*
UNIT 4  TYPE 4  TANK
PARAMETERS 5
.333 1.33 4179. 990. 3237.
INPUTS 5
5,3 5,4 0,0 0,0 0,0
TI MFL 20. 0. TA
DER 1
TI
*
*                        *** OUTPUT ***
*
*  THE SIMULATION OUTPUTS ARE COMPARED TO EXPERIMENTAL
*  DATA BOTH NUMERICALLY AND GRAPHICALLY.
*
UNIT 25  TYPE 25  PRINTER
PARAMETERS 4
.50 0. 12.0 11.
INPUTS 4
9,1 4,1 9,3 5,1
TNKEXP TNKSIM TOUTEX TOUTSI
UNIT 26  TYPE 26  PLOTTER
PARAMETERS 4
.50 0.0 12.0 1.0
INPUTS 4
9,1 4,1 9,3 5,1
TNKEXP TNKSIM TOUTEX TOUTSI
END
```

```
*          ---------- TRNSYS SIMULATION ----------
*
*              *** WITH STORAGE TANK LOAD ***
*
*       THIS TRNSYS DECK IS A SIMULATION OF A THERMAL STORAGE
*   TANK WITH AN IMMERSED COIL. AN EXTERNAL, SENSIBLE HEAT
*   EXCHANGER WITH CONSTANT EFFECTIVENESS IS SUBSTITUTED FOR
*   THE IMMERSED COIL SINCE TRNSYS HAS NO PROVISIONS TO
*   DIRECTLY MODEL AN IMMERSED COIL HEAT EXCHANGER. THE
*   SIMULATION OUTPUT IS COMPARED TO EXPERIMENTAL DATA.
*
*
*                    *** TERMINOLOGY ***
*
*          E = EFFECTIVENESS
*          MFL = IMMERSED COIL MASS (VOLUMETRIC) FLOW RATE
*          TI = INITIAL TANK TEMPERATURE
*          TA = ENVIRONMENT TEMPERATURE
*          TIH = INITIAL TEMPERATURE OF THE FLUID LEAVING
*                THE COIL
*
*                  ** TIME STEP INPUTS ***
*
*          --- TEMPERATURE OF THE WATER ENTERING THE COIL
*          ---- TEMPERATURE OF THE STORAGE TANK REPLACEMENT
*              WATER (DURING A LOAD DRAW ONLY)
*          ----- MASS (VOLUMETRIC) FLOW RATE OF THE LOAD DRAW
*              (DURING A LOAD DRAW ONLY)
*          ---- STORAGE TANK TEMPERATURE (FOR COMPARISON
*              PURPOSES ONLY)
*          ---- TEMPERATURE OF THE WATER LEAVING THE COIL
*              (FOR COMPARISON PURPOSES ONLY)
*
*  SET STARTING TIME, STOPPING TIME AND INTERVAL
*
SIMULATION 0.0 18.0 .1
CONSTANTS E=.267 MFL=450. TI=60.0 TA=23.4 TIH=60.3
*
*  INPUT TEMPERATURE DATA
*
UNIT 9  TYPE 9  DATA READING (FORMATTED)
PARAMETERS 7
4 .50 -1 1 0 0 1
*
*  T(TANK) TCOIL(IN) TCOIL(OUT) T(LOAD)
*
(T3,F4.1,2X,F4.1,2X,F4.1,2X,F4.1)
*
*  INPUT LOAD DRAW MASS FLOW RATE DATA
*
```

```
UNIT 14  TYPE 14  FORCING FUNCTION FOR LOAD MASS FLOW
PARAMETERS 28
0. 0.
.5 0. .5 540. 1.0 540. 1.0 0.
6.5 0. 6.5 270. 7.0 270. 7.0 0.
13.0 0. 13.0 360. 13.5 360. 13.5 0.
17.5 0.
*
*  SENSIBLE HEAT EXCHANGER
*
UNIT 5  TYPE 5  HEAT EXCHANGER
PARAMETERS 4
4 E 4179. 4179.
INPUTS 4
9,2 0,0 4,1 0,0
TI MFL TIH MFL
*
*  THERMAL STORAGE TANK
*
UNIT 4  TYPE 4  TANK
PARAMETERS 5
.341 1.25 4179. 990. 3787.
INPUTS 5
5,3 5,4 9,4 14,1 0,0
TI MFL 20. 0. TA
DER 1
TI
*
*                    *** OUTPUT ***
*
*  THE SIMULATION OUTPUTS ARE COMPARED TO EXPERIMENTAL
*  DATA BOTH NUMERICALLY AND GRAPHICALLY.
*
UNIT 25  TYPE 25  PRINTER
PARAMETERS 4
.50 0. 18.5 9.
INPUTS 4
9,1 4,9 9,3 5,1
TNKEXP TNKSIM TOUTEX TOUTSI
UNIT 26  TYPE 26  PLOTTER
PARAMETERS 4
.50 0.0 18.5 1.0
INPUTS 2
9,1 4,1 9,3 5,1
TNKEXP TNKSIM TOUTEX TOUTSI
END
```

References

1. Holman, J. P., Heat Transfer, McGraw-Hill, Inc., (1976).

2. University of Wisconsin Solar Energy Laboratory, "TRNSYS, a Transient Simulation Program," Engineering Experiment Station Report 38-11, Madison, (1981).

3. Approved Engineering Test Labs., "Performance Test Report on TC 65E Solar-Heatable Water Tank," Tested for Ford Products Corporation, Saugus, Ca., (1978).

4. Vaughn Corp., "Performance Test on the SEPCO Model C80SNR-1 2DHZ Solar Water Heater," Salisbury, ME.

5. Weibelt, J.A., et al., "Free Convection Heat Transfer from the Outside of Radial Fin Tubes," Heat Transfer Engineering, Vol. 1, No. 4, Apr.-June, (1980).

6. Lunde, P. J., Solar Thermal Engineering, John Wiley and Sons, (1980).

7. McAdams, W. H., Heat Transmission, Third Edition, McGraw-Hill, New York, (1954).

8. Horel, J. D. and de Winter, F., "Investigation of Methods to Transfer Heat from Solar Liquid-Heating Collectors to Heat Storage Tanks," Atlas Corporation, Santa Cruz, Ca., (1978).

9. Kreith, F., Principles of Heat Transfer, Third Edition, Intext Press, Inc., New York, (1973).

10. Duffie, J. A. and Beckman, W. A., Solar Engineering of Thermal Processes, Wiley Interscience, New York, 1980.

11. Mitchell, J. C., et al., "FCHART 4.1--A Design Program for Solar Heating Systems," University of Wisconsin-Madison, Engineering Experiment Station Report 50, (1982).